



# Effects of collars in reducing local scour depth around bridge abutments under unsteady flow conditions

Serkan Gokmener<sup>1</sup> · Mustafa Gogus<sup>2</sup> · A. Burcu Altan-Sakarya<sup>1</sup>

Received: 3 January 2024 / Accepted: 20 April 2024

© The Author(s) under exclusive licence to Institute of Geophysics, Polish Academy of Sciences 2024

## Abstract

In this experimental study, semi-circular end collars around semi-circular end abutments and rectangular collars around rectangular abutments were tested in order to investigate the efficiencies of the collars in reducing the local scour depth under unsteady-state clear-water approach flow conditions. Experiments were conducted in a rectangular sediment channel having a sediment pool filled with uniform sand as the bed material. Three different abutment lengths having constant widths were tested under three distinct successive flow intensities that were applied continuously for a duration of 2 h during each experiment. Varying sizes of collars were located at different elevations relative to the bed level. The effect of abutment length, collar width, collar elevation, flow intensity and temporal variation on local scour reduction performances of collars were tested. According to the experimental results, it can be stated that the application of collars around the semi-circular end and rectangular bridge abutments decreases the local scour depth by up to 72% and 51%, respectively. In addition, semi-circular end collars around semi-circular end abutments gave better results in reducing the scour depths than rectangular collars around rectangular abutments. Best collar performances were generally achieved for the largest collar width located around the bed level for semi-circular end abutments and below the bed level for rectangular abutments.

**Keywords** Collar · Rectangular abutments · Scour · Scour countermeasures · Semi-circular end abutments · Unsteady-state flow conditions

## List of symbols

$A_{\text{total}}$	Total area of the abutment with collar on the horizontal plane	$(d_s)_{\text{max}}$	Maximum scour depth at the abutment at the end of the given time duration
$A_{\text{abutment}}$	Abutment area on the horizontal plane	$(d_s)_{\text{max,c}}$	Maximum scour depth at the abutment with collar
$B$	Channel width	$d_{10}$	Sediment size for which 10% of the sediment is finer
$B_a$	Abutment width	$d_{16}$	Sediment size for which 16% of the sediment is finer
$B_c$	Collar width around the abutment	$d_{50}$	Median size diameter
$B_t$	Total width of the abutment width and collar width on horizontal plane	$d_{60}$	Sediment size for which 60% of the sediment is finer
$C_u$	Uniformity coefficient	$d_{84}$	Sediment size for which 84% of the sediment is finer
$d_s$	Final scour depth	$F_r$	Froude number of the flow
		$g$	Gravitational acceleration
		$L_a$	Abutment length
		$R^2$	Correlation coefficient
		$Q$	Discharge of the flow
		$S_0$	Slope of the channel
		$T_c$	Collar thickness
		$t$	Time
		$U$	Mean approach flow velocity

Edited by Prof. Subhasish Dey (ASSOCIATE EDITOR) / Prof. Jochen Aberle (CO-EDITOR-IN-CHIEF).

✉ Serkan Gokmener  
sgokmener11@gmail.com

<sup>1</sup> Hydraulics Laboratory, Department of Civil Engineering, Middle East Technical University, 06800 Ankara, Turkey

<sup>2</sup> Department of Civil Engineering, Çankaya University, 06790 Ankara, Turkey

$U_c$	Value of the $U$ at the threshold of grain motion
$U_*$	Shear velocity of the approach flow
$U_{*c}$	Value of the $U_*$ at the threshold of grain motion
$y$	Flow depth
$y_{0.7}$	Flow depth operated during $U/U_c = 0.7$
$y_c$	Critical flow depth at the threshold of grain motion
$Z_c$	Collar level on the abutment with reference to bed level
$\sigma_g$	Standard deviation of the particle size distribution
$\rho$	Density of the fluid
$\rho_s$	Density of the sediment
$\mu$	Dynamic viscosity of the fluid
$\Theta$	Ratio of the total area of the abutment with collar to the area of the abutment on horizontal plane

## Introduction

The incorporation of bridge components such as abutments and piers within riverbeds for bridge construction induces alterations in river flow patterns through interactions between the fluid and the structures. The presence of these obstacles upstream creates a vertical pressure gradient, a consequence of the stagnation of the approaching flow. This pressure gradient induces a downward flow, primarily responsible for the formation of primary or horseshoe vortices (Barbhuiya and Dey 2004). The downstream side experiences secondary and wake vortices, contributing to the creation of a scour hole through bed material degradation around the bridge elements. The occurrence of scour during flood events poses a significant risk, potentially leading to bridge collapse and loss of lives. According to Richardson and Davis (2001), the collapse of a thousand bridges in the USA over the past three decades has been attributed to extensive scouring that reaches the foundation of bridge elements. Additionally, approximately 30% of bridge failures, as highlighted by Imhof (2004) are associated with natural hazards, particularly events such as floods and scouring. Hence, it is imperative to emphasize the significance of hydraulic design in bridge construction, specifically accounting for scour phenomena, alongside the structural design considerations (Gökmener 2023). In recent decades, several studies have been conducted under steady-state approach flow conditions (Melville 1992; Kandasamy and Melville 1998; Kothiyari and Ranga Raju 2001; Oliveto and Hager 2002; Coleman et al. 2003; Dey and Barbhuiya 2005) and unsteady-state flow conditions (Oliveto and Hager 2005; Hager and Unger 2010; Borghei et al. 2012; Tabarestani and Zarrati 2017; Bombar 2020; Raikar et al. 2022; Gokmener and Gogus 2022) to understand scour mechanism and

predict the temporal variation of maximum scour depth around abutments and piers. Moreover, advanced monitoring techniques in predicting and managing scour around bridge elements have been frequently utilized nowadays. Advanced monitoring techniques are mainly categorized into three groups: monitoring with a reference target, soil–water interface and reverse monitoring. The technique of monitoring with a reference target consists of some methods (magnetic sliding collar, smart rock, etc.) that track the maximum scour depth instantaneously by taking the river bed as the reference point. On the other hand, soil–water interface techniques include monitoring maximum scour depth by using equipment such as sonar, piezoelectric-based sensors, and time-domain reflectometry. Finally, reverse monitoring methods observe the behavior of bridge elements against scouring (Wang et al. 2017). Despite the existence of these extensive studies in the literature, the number of investigations on the temporal development of maximum scour depth around bridge elements is not enough. Consequently, to address issues associated with the scouring process, it is imperative to conduct further research on scour countermeasures and their application on bridge elements (Kumcu et al. 2014). Scour countermeasure techniques can be broadly categorized into two groups: armoring and flow-altering countermeasures (Dey Subhasish et al. 2006). Armoring countermeasures, including riprap, grout-filled bags, cable-tied blocks, and geo-bags, primarily aim to protect bridge elements by preventing scour in critical zones around the structure (Li et al. 2006). In contrast, flow-altering countermeasures, such as collars, vanes, and slots, focus on decreasing the strength of downflow and primary or horseshoe vortices to reduce scour depth and decelerate scour development (Tafarjnoruz et al. 2012). Flow-altering countermeasures are generally considered more cost-effective than armoring countermeasures, primarily due to the reduced amount of stone required, which may not always be readily available at the bridge site (Zarrati et al. 2004). Installation of collars around abutments and piers is one of the most common flow-altering techniques. Collars manipulate the flow pattern around abutments or piers, decreasing the intensity of large bed shear stresses and pressure fluctuations that contribute to scour formation caused by primary vortex and vortex tubes upstream of the bridge elements (Kumcu et al. 2014). Above the collar, downflow movement is decelerated, while the zones below the collar experience reduced downflow and primary vortices. The effectiveness of a collar in reducing scour depends largely on its size and position relative to the bed level (Kumar et al. 1999). In the last decades, several studies have been conducted to investigate the influence of collars in reducing local scour depth around abutments and piers. However, the majority of these extensive studies were focused on the scour reduction efficiency of collars around piers rather than abutments. Zarrati

et al. (2004), Alabi (2006); Moncada-M et al. (2009), Tafarjnoruz et al. (2010, 2012), Wang et al. (2019), Tabarestani and Zarrati (2019), Pandey et al. (2020), Kassem et al. (2023), Mashahir et al. (2024) investigated the scour reduction efficiencies of traditional collars such as rectangular and cylindrical ones while Valela et al. (2021, 2022), Gupta et al. (2023a, 2023b, 2023c) investigated the scour reduction efficiency of recently introduced collar types such as airfoil and streamlined shapes around piers. In addition, Kumar et al. (1999), Grimaldi et al. (2009), Zarrati et al. (2010), Gaudio et al. (2012) tested the combination of collars with other scour countermeasure techniques to enhance scour reduction around bridge piers. Nevertheless, there are a set of studies have been conducted in recent years to examine the influence of collars on abutment scour. Li (2005) revealed that collars successfully reduced scour depth around abutments by preventing the formation of secondary vortices. The optimal performance of collars was observed when placed at an elevation of 0.08 times the flow depth below the bed level. Kumcu et al. (2007) indicated that the maximum scour depth around vertical-wall abutments can be reduced by approximately 20–80% based on the size and location of the collar. Gogus and Dogan (2010) carried out experiments, which are nearly the same as Kumcu et al. (2007, 2014) except for using a bed material with a smaller grain size in order to examine the effect of grain size on scour reduction performances of the collars. The results showed that the grain size of the bed material did not significantly affect the optimal collar elevation. Tekin (2012) stated that collars could reduce the maximum scour depth by around 25–50%, depending on flow intensity, abutment length, collar width, and collar elevation. Kumcu et al. (2014) stated that optimal scour reduction with collars around vertical-wall abutments was generally achieved with larger collar widths positioned below the bed level. Yılmaz (2014) concluded that the installation of collars around spill-through abutments reduces the maximum scour depth by around 52% for both single and multiple abutment configurations. Khosravinia et al. (2018) observed that increased collar width not only reduced the maximum scour depth but also delayed scour formation. The experimental results indicated that the installation of a collar around wing-wall abutments reduces the maximum scour depth by approximately 9–37% with varying collar widths. Hosseinjanzadeh et al. (2021) concluded that the optimal collar location is at the bed level for wing-wall and semi-circular abutments, while below the bed level is optimal for vertical-wall abutments. Gogus et al. (2023) revealed that collar performance in reducing scour increases with wider collars placed below the bed level for a given abutment length. However, they noted that as abutment length increases, collar performance in reducing maximum scour depth decreases, achieving reductions within a range of

9–65% depending on abutment length, collar width, and collar elevation.

The extensive studies discussed above have significantly provided an advanced understanding of collar performance and the key factors influencing it around abutments. However, it is noteworthy that all these investigations were conducted under steady-state clear-water approach flow conditions. The sole exception in the literature, to the best of the authors' knowledge, conducted under unsteady-state approach flow conditions is the study by Tabarestani and Zarrati (2019). In their study, the time for reaching the scour below the collar level was considered rather than scour reduction amounts of collars to evaluate the scour reduction efficiency of collars. The results indicated that decreasing flow intensity from 0.99 to 0.8 delayed the onset of degradation of the bed material below the collar by 26 times. Hereby, it was stated that flow intensity is the most dominant parameter for scour development around piers either without or with collars. Despite the wealth of information provided by existing studies, a detailed investigation into the influence of collars on scour development around bridge elements under unsteady-state approach flow conditions is notably lacking. The complexity of the experimental procedure, characterized by rapid variations in flow parameters, coupled with the challenge of deriving a generalized formula for predicting scour depth, has hindered a more comprehensive investigation of collar effectiveness in such dynamic conditions (Oliveto and Hager 2005). For that reason, the effect of flow variation on scour development and the behavior of scour countermeasures against scour formation must be studied in more detail to understand scour formation under unsteady-state approach flow conditions. In the scope of the present study, experiments were conducted to investigate scour reduction efficiencies of collars under unsteady-state clear-water approach flow conditions. Collars of varying sizes and at different elevations relative to the bed level were attached to abutments of various lengths. Unsteadiness was introduced through the utilization of a stepwise hydrograph, incorporating three distinct flow intensities, each applied continuously for a duration of 2 h.

## Materials and methods

### Experimental setup

Experiments were carried out in a rectangular sediment channel with plexiglass side walls having 28.5 m in length and 1.5 m in width, with a slope of  $S_0 = 0.001$  (Figs. 1 and 2).

The sand layer, extending 5.8 m in the flow direction with a depth of 0.48 m, was located 13.5 m away from the upstream of the channel. This sand layer comprised uniform

**Fig. 1** Sketch of the experimental setup (Gogus et al. 2023)

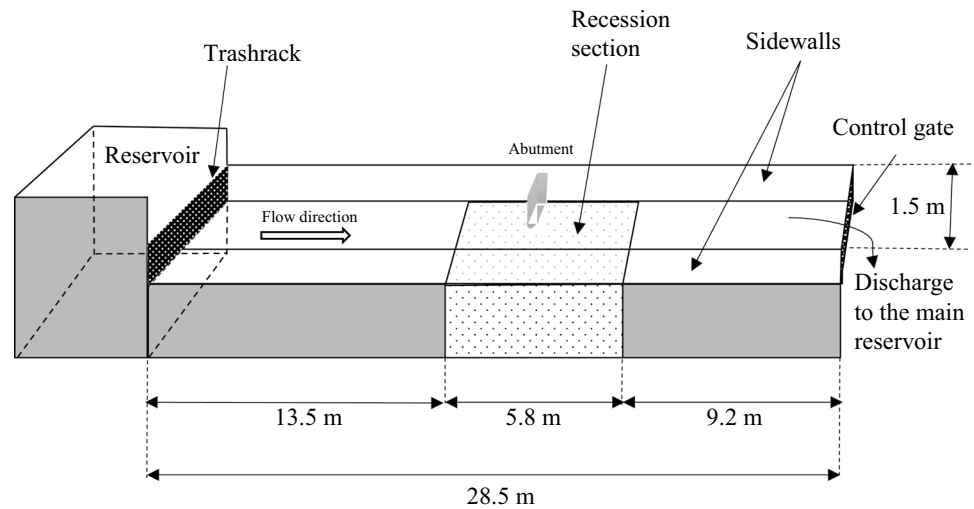


**Fig. 2** View of the experimental setup from downstream

sand characterized by a median diameter of  $d_{50} = 1.5$  mm, standard deviation of the particle size distribution of  $\sigma_g = 1.29$  and uniformity coefficient of  $C_u = d_{60}/d_{10} = 1.7$  where  $d_{60}$  and  $d_{10}$  are the sediment sizes for which 60% and 10% of the sediment is finer, respectively. Since scour reduction performances of the collars have been obtained almost

the same for varying sediment sizes (Kumcu et al. 2014), in this study, it was decided to carry out experiments with one sediment size. The hydraulic system utilized a constant-head tank equipped with a pump boasting a discharge capacity of 250 l/s to provide the required flow to the channel. The targeted flow depth and velocity were achieved by adjusting

the control gate at the end of the channel. Discharge measurement, with an accuracy of  $\pm 2\%$ , was facilitated by an electromagnetic flowmeter attached to the intake pipe. Turbulence reduction measures included the passage of flow through a sharp-crested rectangular weir (1.5 m wide and 0.3 m deep), an energy dissipater pool, and a sheet-iron strainer at the channel entrance. Flow depth measurements were taken using a ruler affixed to the sand layer wall, with an accuracy of  $\pm 1$  mm. Maximum scour depths at the conclusion of the experiments were determined using a point gauge, accurate to  $\pm 1$  mm.

### Abutment and collar models

In the experiments, abutments of 3 different lengths,  $L_a = 20$  cm, 30 cm and 40 cm, fabricated from plexiglass, were tested. Since the effect of abutment width,  $B_a$ , on the scour hole development is insignificant (Oliveto and Hager 2002; Kumcu et al. 2007), abutment widths were kept constant at 10 cm along the experiments. As a scour countermeasure, plexiglass collars with widths of  $B_c = 5$  cm, 7.5 cm, and 10 cm having 3 mm thicknesses were tested in the experiments. The collars were located around the abutment at  $Z_c/y_{0.7} = -0.50, -0.25, \pm 0.00$ , where  $Z_c$  is the collar elevation relative to the bed level and  $y_{0.7}$  is the flow depth of the experiment having the flow intensity of  $U/U_c = 0.7$ . However, the collars placed at the elevation of  $Z_c/y_{0.7} = -0.50$  for the abutment lengths of  $L_a = 20$  cm were not tested in the experiments since the obtained dimensionless maximum

scour depths for these abutments did not reach to the elevation of  $Z_c/y_{0.7} = -0.50$ .

A sketch of the abutment model with the attachment of a collar is given in Fig. 3.

Abutment lengths, collar sizes and locations during the experiments are listed with a sketch of a semi-circular end bridge abutment and collar arrangement in Table 1.

### Dimensional analysis

The maximum scour depth around an abutment with a collar,  $(d_s)_{\max,c}$ , under unsteady-state clear-water approach flow conditions are presented as a function of parameters given as follows:

$$(d_s)_{\max,c} = f\{L_a, B_a, B_c, Z_c, T_c, U, y, S_0, g, \rho_s, \rho, \mu, d_{50}, \sigma_g, t, t_p, B\}, \quad (1)$$

where  $L_a$  is the length of the abutment perpendicular to the flow direction,  $B_a$  is the width of the abutment;  $B_c$  is the collar width;  $Z_c$  is the elevation of the collar with respect to the sand level;  $T_c$  is the collar thickness;  $U$  is the average flow velocity;  $y$  is the flow depth;  $S_0$  is the bed slope of the channel;  $g$  is the acceleration of gravity;  $\rho_s$  is the density of bed material;  $\mu$  is the dynamic viscosity of water;  $d_{50}$  is the median diameter of bed material;  $\sigma_g$  is the geometric standard deviation of bed material and  $\sigma_g$  is the  $d_{84}/d_{16}$  where  $d_{84}$  is the particle diameter for which 84% of the sediment is finer; and  $d_{16}$  is the particle diameter for which 16% of the sediment is finer;  $t$  is the time period of the experiment for

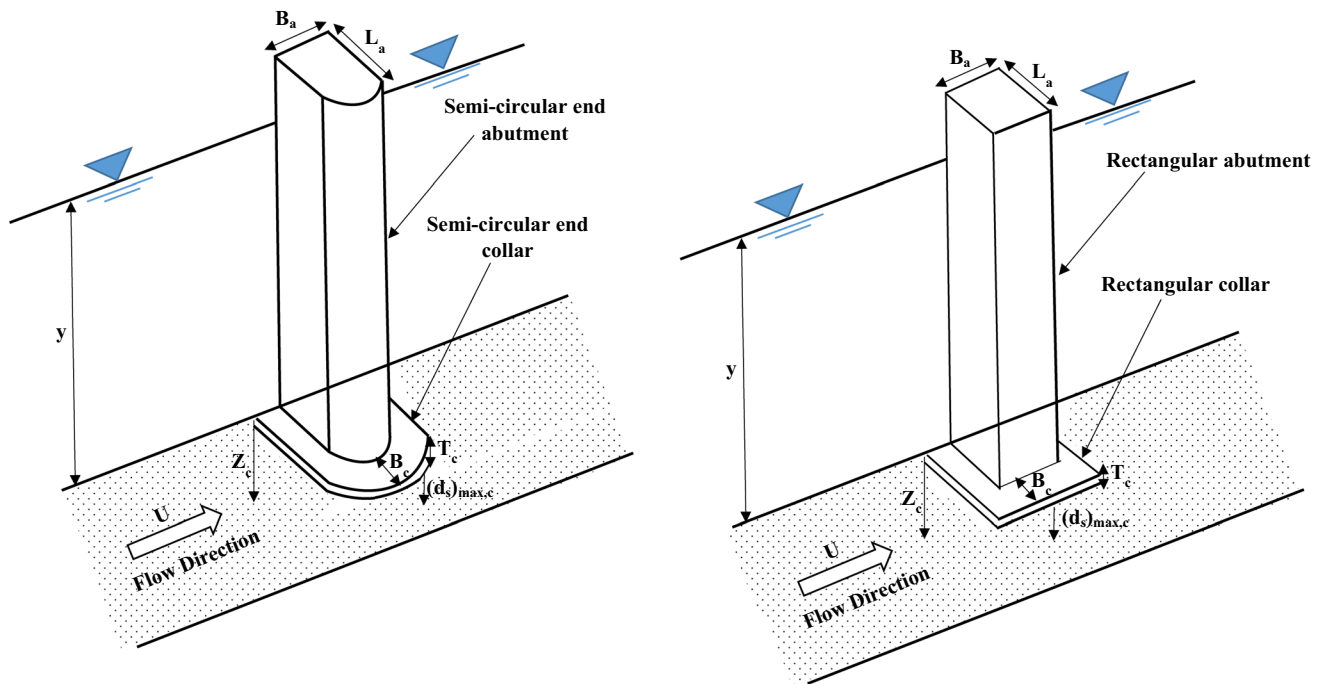
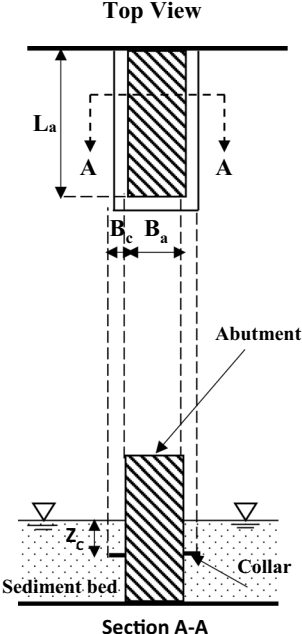


Fig. 3 Sketch of the abutment-collar arrangement for semi-circular end and rectangular abutments

**Table 1** Abutment lengths, collar sizes and locations tested during the experiments

Abutment type	$L_a$ (cm)	$B_c$ (cm)	$Z_c$ (cm) with respect to the bed level	$Z_c/y_{0.7}$ with respect to the bed level
	40	10.0	-8.70	-0.50
			-4.35	-0.25
			±0.00	±0.00
			-8.70	-0.50
			-4.35	-0.25
			±0.00	±0.00
	30	10.0	-8.70	-0.50
			-4.35	-0.25
			±0.00	±0.00
			-8.70	-0.50
			-4.35	-0.25
			±0.00	±0.00
20	10	-4.35	-0.25	
		±0.00	±0.00	
		-4.35	-0.25	
		±0.00	±0.00	
		-4.35	-0.25	
		±0.00	±0.00	

a given flow intensity starting from the beginning as 2 h, 4 h and 6 h duration of the experiment;  $t_p$ , which equals to 6 h in this study, is the total duration of the experiment that represents the total duration of flood and  $B$  is the width of the channel.

The parameters given in Eq. (2) are transformed into dimensionless terms by applying Buckingham's  $\pi$  theorem as follows:

$$\frac{(d_s)_{\max,c}}{y} = f \left\{ \frac{L_a}{y}, \frac{B_a}{y}, \frac{B_c}{y}, \frac{Z_c}{y}, \frac{T_c}{y}, \frac{\rho_s}{\rho}, \frac{U}{\sqrt{gy}}, \frac{B}{y}, \frac{\mu}{U\rho y}, \frac{Ut}{y}, \frac{t}{t_p}, S_0, \sigma_g, \frac{d_{50}}{y} \right\}. \quad (2)$$

Since the experiments were conducted with one sediment size, and some other parameters—bed slope, channel width, collar thickness and abutment width—are constant, the related parameters can be excluded from Eq. (3). In

addition, considering the turbulence nature of open channel flows, viscous effects can also be neglected. Moreover, the flow intensity term,  $U/U_c$  can be written instead of the Froude number,  $U/\sqrt{gy}$ . Therefore, Eq. (3) can be simplified as follows:

$$\frac{(d_s)_{\max,c}}{y} = f \left\{ \frac{L_a}{y}, \frac{L_a}{B_c}, \frac{Z_c}{y}, \frac{U}{U_c}, \frac{Ut}{y}, \frac{t}{t_p} \right\}. \quad (3)$$

The performances of collars on scour reduction were calculated by comparing scour depths of a given abutment with and without collar cases using the expression given in Eq. (4):

$$\frac{(d_s)_{\max} - (d_s)_{\max,c}}{(d_s)_{\max}} = f \left\{ \frac{L_a}{y}, \frac{L_a}{B_c}, \frac{Z_c}{y}, \frac{U}{U_c}, \frac{Ut}{y}, \frac{t}{t_p} \right\}, \quad (4)$$

where  $(d_s)_{\max}$  is the maximum scour depth around the abutment without a collar.

## Flow conditions

In scouring studies, flow intensity is typically characterized by either the ratio of shear velocities,  $U_*/U_{*c}$ , or the ratio of mean velocities  $U/U_c$  (Li et al. 2006). In this study, the flow depth required to have clear-water flow conditions was determined by using the ratio of  $U/U_c$ , where  $U$  is the average velocity of the approach flow and  $U_c$  is the value of  $U$  at the threshold of grain motion (Li et al. 2005; Kumcu et al. 2007, 2014; Khosravinia et al. 2018). Prior to beginning the tests, preliminary experiments were carried out in the channel without an abutment to estimate the necessary water depth and discharge by monitoring the initiation of grain motion. From these experiments, the critical water depth and the mean approach flow velocity were observed as  $y_c = 12.1$  cm and  $U_c = 0.3736$  m/s, respectively, when the discharge was  $Q = 0.0678$  m<sup>3</sup>/s. Critical shear velocity was also calculated theoretically from Shield's diagram by using the equation proposed by Melville and Coleman (2000), in which the units of the parameters  $U_{*c}$  and  $d_{50}$  are (m/s) and (mm), respectively:

$$U_{*c} = 0.0305 \sqrt{d_{50}} - \frac{0.0065}{d_{50}}. \quad (5)$$

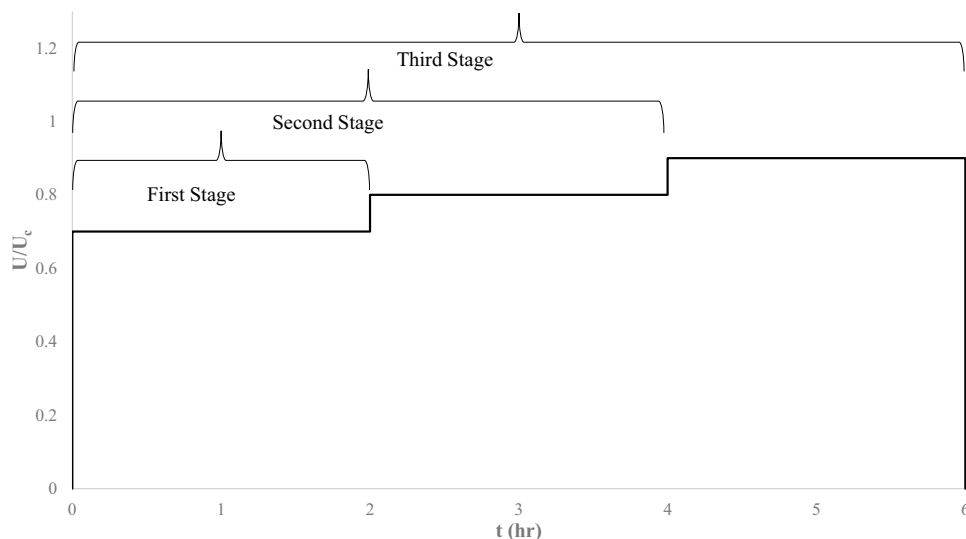
The critical shear velocity was calculated as 0.032 and 0.033 m/s from the experimental and theoretical approaches, respectively. Thus, for the discharge of  $Q = 0.0678$  m<sup>3</sup>/s, the flow depth values to obtain flow intensities of  $U/U_c = 0.7$ , 0.8 and 0.9 were calculated as  $y = 17.4$  cm, 15.2 cm and 13.5 cm, respectively.

## Experimental procedure

Before each experiment, the sand layer was carefully compressed and leveled to ensure a smooth and homogeneous bed surface. A small discharge was introduced into the flume to prevent any disturbance to the surface of the sediment layer. Once the flow reached the tailgate of the channel, the discharge was gradually raised until it reached the desired value ( $Q = 0.0678$  m<sup>3</sup>/s). Simultaneously, adjustments were made to the tailwater gate downstream to achieve the desired flow depth ( $y = 17.4$  cm) and flow intensity ( $U/U_c = 0.7$ ). After the flow depth had been stabilized, the experiments were initiated. A stepwise hydrograph based on flow intensity was applied using a constant discharge ( $Q = 0.0678$  m<sup>3</sup>/s) for a duration of 6 h. The flow intensity was systematically increased at 2-h intervals, transitioning from 0.7 ( $y = 17.4$  cm) to 0.8 ( $y = 15.2$  cm), and subsequently to 0.9 ( $y = 13.5$  cm). To avoid disrupting the flow pattern and scour hole during experiments, scour depth measurements could not be done during the experiments. Additionally, measuring scour depths below the collar level was impractical without detaching the collar. Therefore, each experiment was divided into three stages. (Fig. 4).

In the first stage, the flow intensity of  $U/U_c = 0.7$  was tested only for 2 h, then the experiment was ended and scour measurements were done after the drain of water from the channel. In the second stage,  $U/U_c = 0.7$  were tested for 2 h, then the flow intensity was gradually increased to  $U/U_c = 0.8$  and the experiment was continued for another 2 h and then was ended. So, scour depth measurements were done at the end of the 4th hour. The same procedure was repeated in the third stage with the flow intensity of  $U/U_c = 0.9$  for another 2 h. After completing the third stage, the final scour

**Fig. 4** Stepwise hydrograph used in the experiments with the divided stages



depths at the end of each stage, the 2nd, 4th and 6th hours, were achieved. According to literature focusing on equilibrium scour depth, it is generally acknowledged that approximately 50 h are required to reach such a state (Farshad et al. 2022). However, in real flood cases, the duration of the flood event is often shorter than the time needed to attain equilibrium scour conditions. Consequently, the magnitude of maximum scour depths resulting from floods tends to be less than those corresponding to equilibrium cases (Cao and Gu 2015; Gu et al. 2020; Shampa et al. 2020). Therefore, experiments conducted under steady-state approach flow conditions to achieve equilibrium scour depth may tend to overestimate scour depth in flood conditions. Furthermore, researchers such as Khosravinia et al. (2018), Pandey et al. (2020) and Tekin (2012) underlined that approximately 70–75% of equilibrium scour depth is developed within a time frame of less than 2 h. Also, Melville and Chiew (1999) have asserted that 50–80% of the maximum scour depth is reached at around 10% of the equilibrium time. By the way,

the primary objective of the present study is to investigate the scour reduction efficiencies of collars with varying size and elevation configurations rather than investigating the maximum scour depth at equilibrium conditions. Therefore, the selected experimental duration of 6 h was found to be sufficient in the experiments to assess the scour reduction performances of collars (Johnson et al. 2001; Kumcu et al. 2007, 2014; Valela et al. 2022).

The experimental conditions of the experiments are listed in Table 2.

## Analysis and discussion of the experimental results

Within the scope of this study, 162 experiments, 18 of them without collars, were conducted with constant discharge and decreasing flow depth (increasing flow velocity and intensity) for various flow intensities, abutment lengths, collar widths and

**Table 2** Summary of the experimental conditions (SC = Semi-circular end abutment, RC = Rectangular abutment)

Experiment No	$L_a$ (cm)	$Q$ (l/s)	$t$ (hrs)	$y$ (cm)	$U$ (m/s)	$F_r$	$U_c$ (m/s)	$U/U_c$
SC1	40	67.8	0–2	17.4	0.262	0.2	0.3736	0.7
RC1			2–4	15.2	0.299	0.24	0.3736	0.8
			4–6	13.5	0.336	0.29	0.3736	0.9
SC2	30	67.8	0–2	17.4	0.262	0.2	0.3736	0.7
RC2			2–4	15.2	0.299	0.24	0.3736	0.8
			4–6	13.5	0.336	0.29	0.3736	0.9
SC3	20	67.8	0–2	17.4	0.262	0.2	0.3736	0.7
RC3			2–4	15.2	0.299	0.24	0.3736	0.8
			4–6	13.5	0.336	0.29	0.3736	0.9

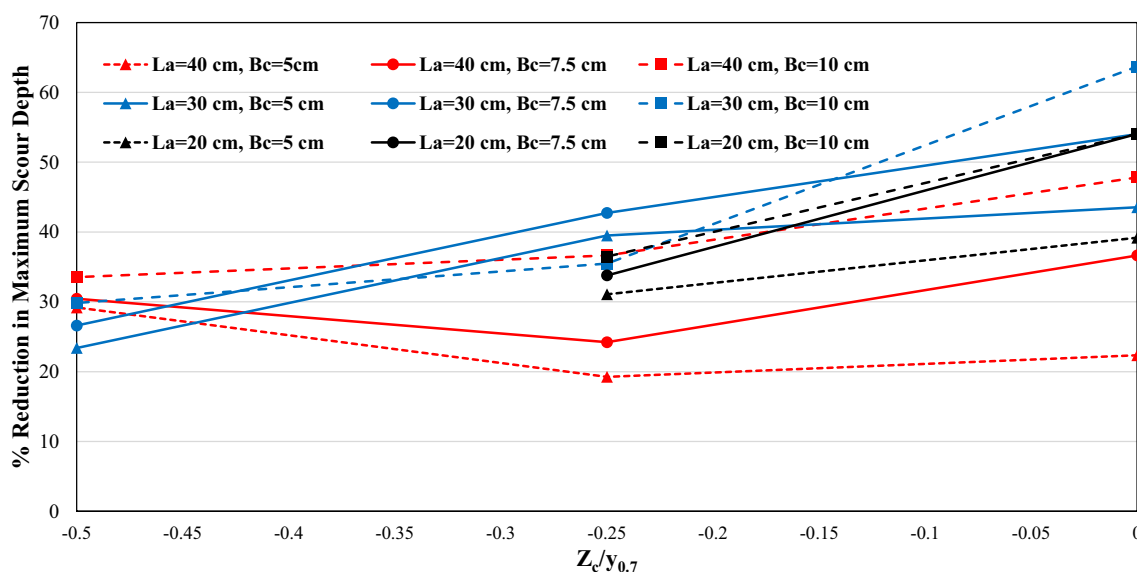


**Fig. 5** Effect of collar size and elevation on the maximum scour depth around semi-circular end abutments ( $t=6$  h)



locations. In the experiments, a stepwise hydrograph having a total time duration of 6 h was applied with collars to investigate the performances of collars as a scour countermeasure.

### Semi-circular end bridge abutments

Since the temporal change of maximum scour depth is not analyzed in this section, only the final stages of the experiments are presented and discussed. Figure 5 illustrates the effect of abutment length, collar size, and elevation on the maximum scour depth around all tested semi-circular end abutment lengths in this study.

At the end of the third stage of the experiments, the most effective collar performances in reducing the scour depths were obtained for the abutment of length  $L_a = 30$  cm regardless of the collar size and while the least effective performances were noted for the abutment of length  $L_a = 40$  cm. However, when the collars were positioned at the elevation of  $Z_c/y_{0.7} = -0.50$ , the performances of the collars were better for the abutment of length  $L_a = 40$  cm than that of  $L_a = 30$  cm aligning with trends observed in the first and second stages of the experiments. In conclusion, it can be stated that at a small flow intensity value ( $U/U_c = 0.7$ ,  $t = 2$  h) the longest abutment,  $L_a = 40$  cm, with the largest collar size,  $B_c = 10$  cm, yields the maximum scour reduction of 72% at the collar elevation of  $Z_c/y_{0.7} = \pm 0.00$ . As the value of  $Z_c/y_{0.7}$  gets smaller,  $-0.25$  and then  $-0.50$ , the corresponding maximum scour reductions exhibited a decreasing trend. The best collar location regarding the maximum scour reduction remained at the bed level,  $Z_c/y_{0.7} = \pm 0.00$ , as the flow intensity increased ( $U/U_c = 0.8$ ,  $t = 4$  h and  $U/U_c = 0.9$ ,  $t = 6$  h). However, the long abutments experienced greater scour than the short ones, leading to a reduction in performance of collars around the abutment of  $L_a = 40$  cm decreased compared to other abutment lengths tested as the flow intensity increased.

The effect of collar size and flow intensity on the maximum scour depth around all the semi-circular end abutment lengths tested in this study is depicted in Fig. 6. When collars were placed at the elevation of  $Z_c/y_{0.7} = \pm 0.00$  except the zone of  $U/U_c$  between 0.7 and 0.8 for abutments of lengths  $L_a = 20$  cm and 30 cm, the scour reduction efficiencies of the collars for a given abutment length decrease with increasing  $U/U_c$ . At the end of the first stage of the experiment with the flow intensity of 0.7, the maximum scour reductions were observed within a range of 62.50–71.88% for the abutment of length  $L_a = 40$  cm. However, at the end of the third stage of the experiment with the flow intensity of 0.9, smaller scour reduction efficiencies, within the range of 22.36–47.83%, were observed around the abutment of length  $L_a = 40$  cm for the collar sizes tested.

At the elevation of  $Z_c/y_{0.7} = -0.25$ , the efficiency of the collars in reducing scour depths decreased for the abutment

of length  $L_a = 40$  cm with increasing flow intensity. Conversely, for the other tested abutment lengths, there was a general trend of increased collar performance with higher flow intensity. At the end of the first stage, the most effective collar performances were recorded for the abutment of length  $L_a = 40$  cm. However, at the end of the third stage, significantly lower collar performances were observed for the abutment of length  $L_a = 40$  cm for a given collar size. Particularly for the shortest abutment of length  $L_a = 20$  cm tested in this study, a remarkable increase in collar performance was noted during the second and third stages of the experiments. Furthermore, the collar efficiency was better for the abutment of length  $L_a = 20$  cm when compared to  $L_a = 40$  cm during this period. The maximum scour reductions were observed within a range of 35.48–42.74% at the end of the third stage for the abutment of length  $L_a = 30$  cm.

When collars were positioned at the elevation of  $Z_c/y_{0.7} = -0.50$ , the scour reduction performances of the collars attached to the abutment of length  $L_a = 40$  cm surpassed that of the abutment of length  $L_a = 30$  cm for a given collar size during the experiments. However, as the scour depths increased with increasing flow intensity and time, the scour reduction performances of the collars attached to the abutment lengths of  $L_a = 30$  and 40 cm started to converge with each other. In other words, as the scouring rate increased, collars started to give better performances as the abutment length decreased. In summary, the efficacy of the collars generally increased with an increase in collar size, independent of abutment length. Larger collars offer enhanced protection against vortices, resulting in smaller scour holes compared to smaller collars, making it more challenging for vortices to reach deeper elevations. During the initial stages of the experiments, scour formation did not extend to the level of  $Z_c/y_{0.7} = -0.5$  and  $-0.25$ , so those collars did not exhibit significant effects in reducing scour depth. Moreover, the scour reduction performances of the collars located at  $Z_c/y_{0.7} = -0.5$  and  $-0.25$  increased with increasing flow intensity and time due to the penetration of vortices to deeper locations, resulting in larger scour depths. Consequently, collars placed below the bed level would be effective in circumstances with greater scour depth potentials, such as higher flow intensity, time, and abutment length.

### Rectangular bridge abutments

In Fig. 7, the effect of collar size and elevation on the maximum scour depth around all the rectangular abutment lengths tested in this study is illustrated using the data of third stage experiments.

At the end of the third stage of the experiments, it can be stated that the efficiency of collars decreased with increasing abutment length for a given collar elevation. At the elevation of  $Z_c/y_{0.7} = -0.25, \pm 0.00$ , the performance of the collar of

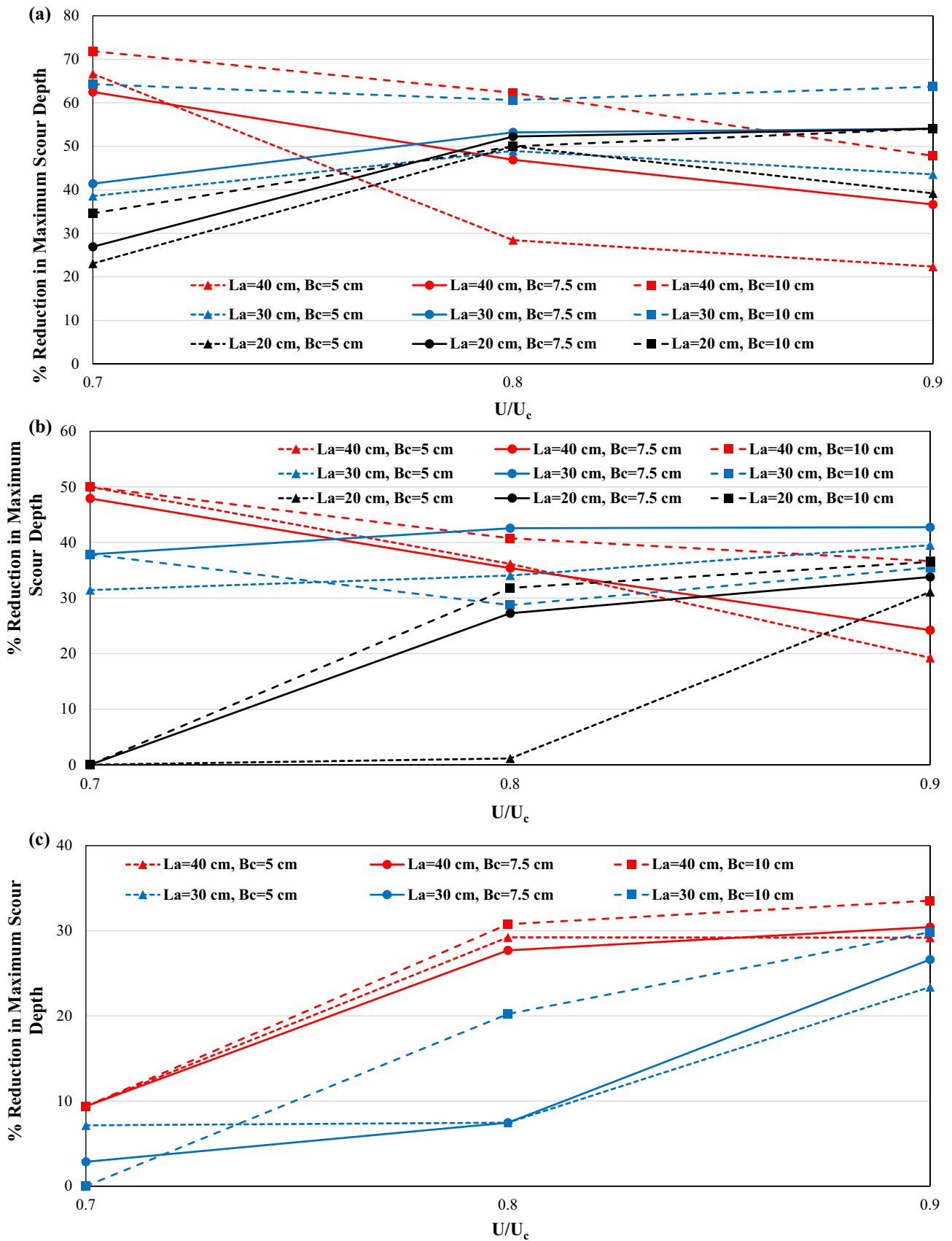


**Fig. 6** **a** Effect of collar size and flow intensity on the maximum scour depth around semi-circular end abutments for  $Z_c/y_{0.7} = \pm 0.00$ . **b** Effect of collar size and flow intensity on the maximum scour depth around semi-circular end abutments for  $Z_c/y_{0.7} = -0.25$ . **c** Effect of collar size and flow intensity on the maximum scour depth around semi-circular end abutments for  $Z_c/y_{0.7} = -0.50$

$B_c = 10$  cm that attached to the abutments of lengths  $L_a = 20$  and 30 cm were nearly identical while the efficiencies of the collars of  $B_c = 5$  and 7.5 cm gave better results in reducing the maximum scour depth around the abutment of length  $L_a = 20$  cm than  $L_a = 30$  cm. At the end of the 6 h, the best collar performances were obtained for the abutment of length  $L_a = 30$  cm having a collar size of  $B_c = 10$  cm and the worst ones were observed for the abutment of length  $L_a = 40$  cm with  $B_c = 5$  cm.

The effect of collar size and flow intensity on the maximum scour depth around all the rectangular abutment lengths examined in this study is depicted in Fig. 8. Except for some abutment-collar arrangements;  $L_a = 30$  cm with  $B_c = 7.5$  cm and 10 cm, and  $L_a = 20$  cm with  $B_c = 5$  cm and 7.5 cm in the zone of  $U/U_c$  between 0.7 and 0.8, scour reduction performances decreased as  $U/U_c$  increased for all cases tested in this study for a given abutment length and collar size when collars were placed at the elevation of  $Z_c/y_{0.7} = \pm 0.00$ . The efficiency of collars decreased as the abutment length increased with increasing flow intensity and time. At the end of the first and second stages of the experiments with the flow intensities of 0.7 and 0.8, respectively, the efficiencies of the collars did not exhibit significant differences for the

abutment lengths of  $L_a = 20$  and 30 cm. However, for the abutment of length  $L_a = 40$  cm, the collar efficiencies experienced a notable decrease. Between the 4th and 6th hours of the experiment with the flow intensity of 0.9, the efficiencies of the collars for the longer abutments of lengths  $L_a = 30$  and 40 cm decreased while for the shorter abutment of length,  $L_a = 20$  cm increased.

At the elevation of  $Z_c/y_{0.7} = -0.25$ , making conclusive remarks about the effect of abutment length on the scour reduction performances of the collars was challenging at the end of the first and second stages of the experiments. During these phases, the maximum scour reductions were recorded for the abutments of lengths  $L_a = 30$  and 40 cm having a collar of  $B_c = 10$  cm, respectively. However, between the 4th and 6th hours of the experiments, the efficiencies of the collars attached to the abutment of length  $L_a = 40$  cm witnessed a significant decline with increasing flow intensity, resulting in the worst scour reductions for this abutment length for a given collar size. Furthermore, the maximum scour reductions for a given collar size were noted for the shortest abutment of length  $L_a = 20$  cm except in the case of  $U/U_c = 0.7$ . Consequently, it can be inferred that the efficiencies of the collars diminished as the abutment length increased during periods of high flow intensities. When collars were tested at the elevation of  $Z_c/y_{0.7} = -0.50$ , the scour reduction performances of the collars attached to the abutment of length  $L_a = 40$  cm were generally better than the abutment of length  $L_a = 30$  cm for a given collar size. However, after the 4th hour of the experiments, when the flow intensity value increased to 0.9, the collars became more efficient for

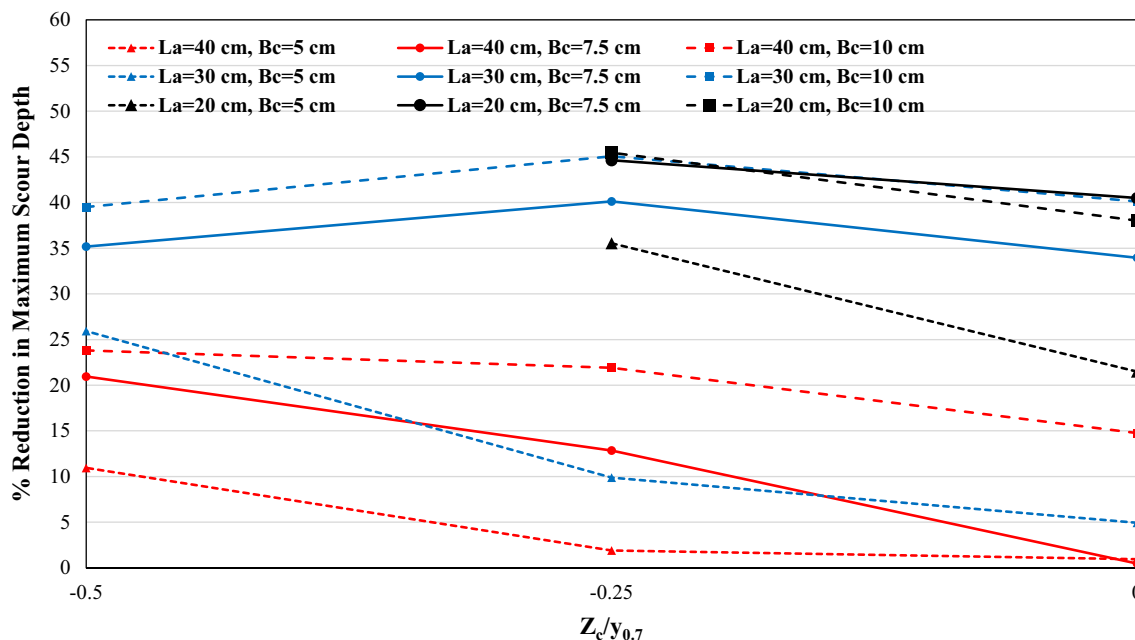


**Fig. 7** Effect of collar size and elevation on the maximum scour depth around rectangular abutments ( $t=6$  h)

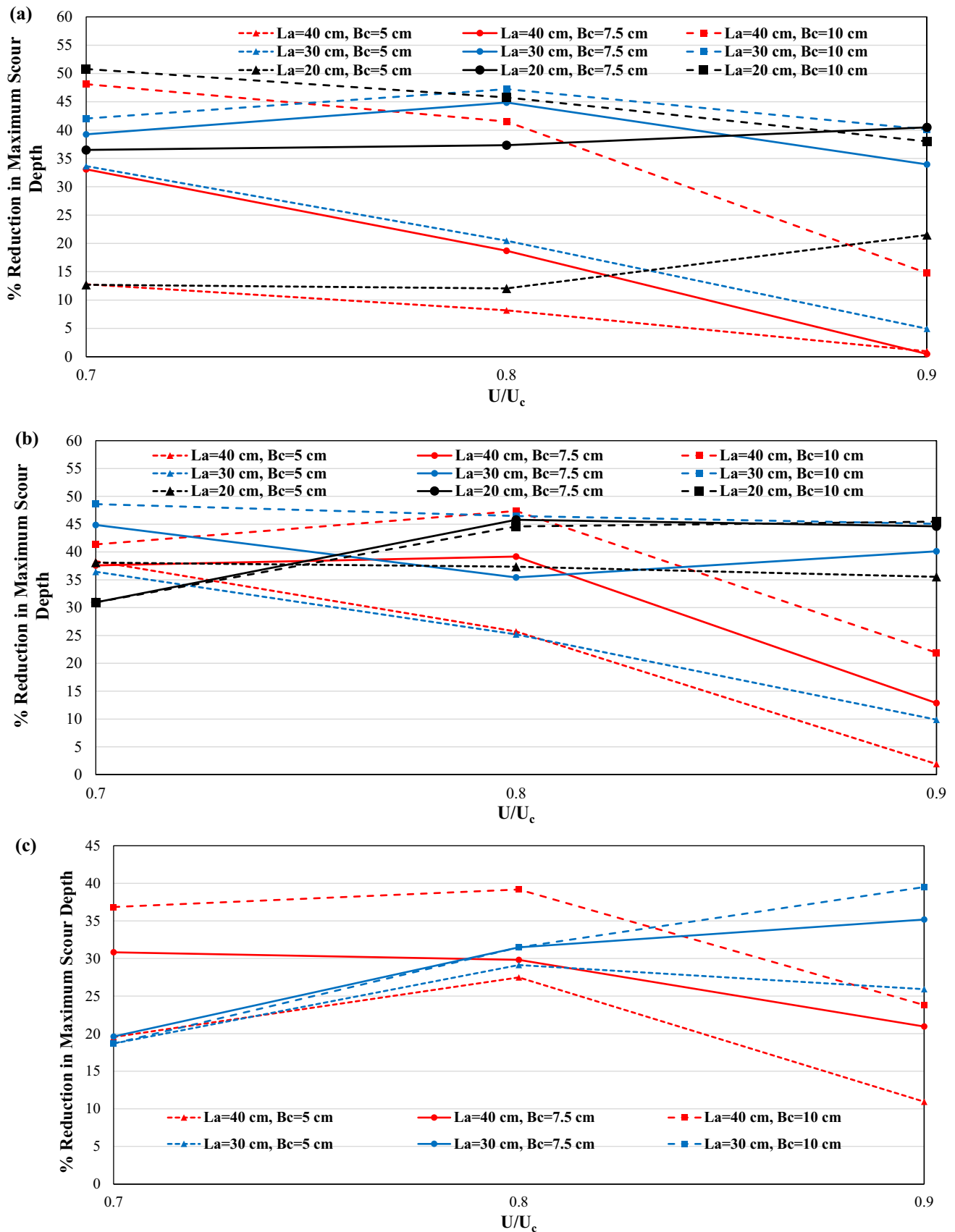


**Fig. 8** **a** Effect of collar size and flow intensity on the maximum scour depth around rectangular end abutment for  $Z_c/y_{0,7} = \pm 0.00$ . **b** Effect of collar size and flow intensity on the maximum scour depth around rectangular end abutment for  $Z_c/y_{0,7} = -0.25$ . **c** Effect of collar size and flow intensity on the maximum scour depth around rectangular end abutment for  $Z_c/y_{0,7} = -0.50$

the abutment of length  $L_a = 30$  cm. Between the 4th and 6th hours, the efficiencies of the collars attached to the abutment of length  $L_a = 40$  cm dramatically decreased while  $L_a = 30$  cm increased. Thus, based on the experimental results, it can be revealed that as the scouring rate increased, collars started to be more effective as the abutment length decreased.

In summary, collars with larger widths demonstrated greater effectiveness in minimizing the maximum scour depth around abutments, regardless of the abutment length. This is attributed to the enhanced protective capacity of larger collars against vortices, resulting in the creation of smaller scour holes compared to those associated with smaller collars. Throughout the experiments, the maximum scour reductions were generally observed when the collars were placed at the elevation of  $Z_c/y_{0,7} = -0.25$ . However, during the initial stages of the experiments with the flow intensity of 0.7, for the abutment of length  $L_a = 20$  cm the maximum scour reductions were recorded at the elevation of  $Z_c/y_{0,7} = \pm 0.00$  and at the end of the third stage of the experiments, for the abutment of length  $L_a = 40$  cm, the maximum scour reductions were recorded at the elevation of  $Z_c/y_{0,7} = -0.50$ . Since the scour formation was greater around the abutment of length  $L_a = 40$  cm than those of  $L_a = 20$  cm, the

scour formation reached into the deeper locations below the bed level and the maximum scour depth increased with increasing flow intensity and time. Hence, the collars that were placed at the elevation of  $Z_c/y_{0,7} = -0.50$  gave better results in reducing the maximum scour depth around longer abutment lengths such as  $L_a = 40$  cm having higher flow intensity value and duration,  $U/U_c = 0.9$  and  $t = 6$  h, while the collars at the elevation of  $Z_c/y_{0,7} = \pm 0.00$ , gave better results around shorter abutment lengths such as  $L_a = 20$  cm having smaller flow intensity and test duration,  $U/U_c = 0.7$ ,  $t = 2$  h.

### Comparison of the scour reduction performances of the collars around semi-circular end and rectangular bridge abutments

The comparison of the scour reduction efficiencies for both semi-circular end and rectangular collars attached to semi-circular end and rectangular abutments, respectively, is presented in this subsection. In the related figures, semi-circular end and rectangular abutments are denoted as SC and RC, respectively.

In Fig. 9, a comparative analysis is presented regarding the scour reduction performances of various collar sizes and elevations around semi-circular end and rectangular abutments of length  $L_a = 40$  cm is presented.

At the end of the third stage of the experiments, regardless of the collar elevations, whether at the bed level or below it, semi-circular collars attached to semi-circular end abutments exhibited greater efficiency than rectangular

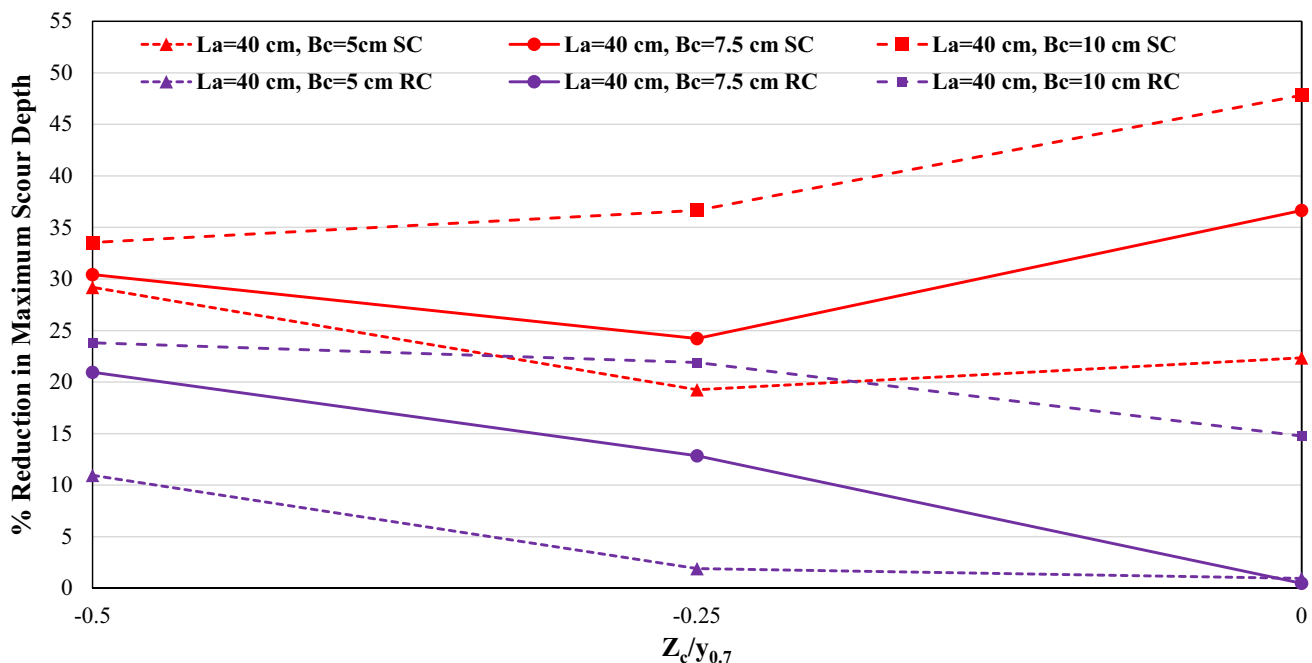


**Fig. 9** Comparison of the effects of collar size and elevation on the maximum scour depth around semi-circular end and rectangular abutments of length  $L_a = 40$  cm ( $t = 6$  h)

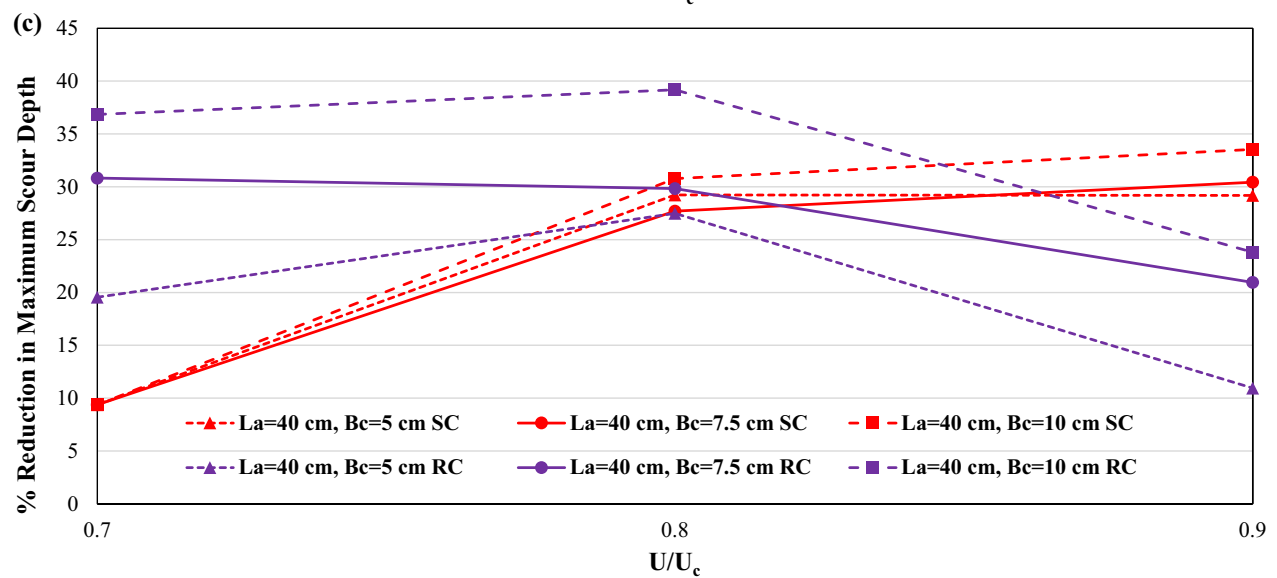
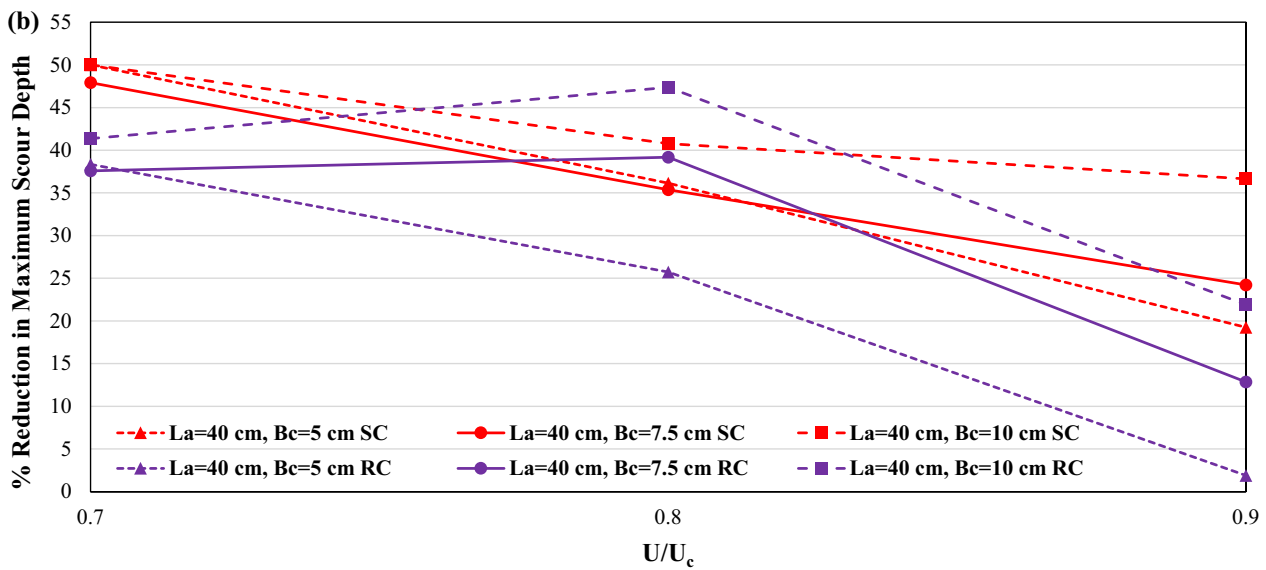
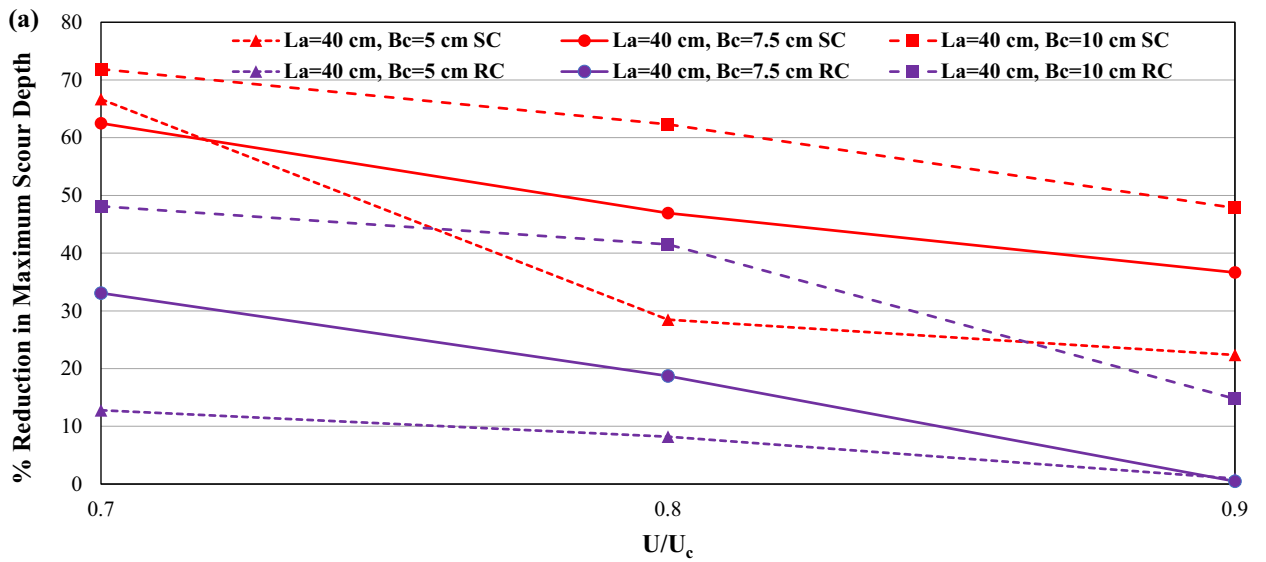


**Fig. 10** **a** Comparison of the effect of collar size and flow intensity on the maximum scour depth around semi-circular end and rectangular abutments of  $L_a=40$  cm for  $Z_c/y_{0.7}=\pm 0.00$ . **b** Comparison of the effect of collar size and flow intensity on the maximum scour depth around semi-circular end and rectangular abutments of  $L_a=40$  cm for  $Z_c/y_{0.7}=-0.25$ . **c** Comparison of the effect of collar size and flow intensity on the maximum scour depth around semi-circular end and rectangular abutments of  $L_a=40$  cm for  $Z_c/y_{0.7}=-0.50$

collars attached to rectangular abutment for a given collar width. Nonetheless, it should be noted that the efficiencies of the semi-circular end and rectangular collars converged with each other when the collars were placed deeper into the bed material. In other words, the efficiencies of the rectangular collars attached to the rectangular abutment are found to be more effective below the bed level. As a final comment, it can be underlined that at the end of each stage, semi-circular end collars attached to the semi-circular end abutment showed better performances compared to rectangular collars attached to the rectangular abutment almost at any  $Z_c/y_{0.7}$  value tested. The best efficiencies in reducing the maximum scour depth were attained when the collars were placed at the bed level,  $Z_c/y_{0.7}=\pm 0.00$ .

In Fig. 10, the comparative analysis of the scour reduction performances of various collar sizes and flow intensities around semi-circular end and rectangular abutments of length  $L_a=40$  cm is depicted. When the collars were placed at the elevation of  $Z_c/y_{0.7}=\pm 0.00$ , the scour reduction performances of the semi-circular end collars attached to the semi-circular abutment were observed greater than the rectangular collars attached to the rectangular abutment at any flow intensity tested, except the case of  $L_a=40$  cm with  $B_c=10$  cm for  $U/U_c=0.8$ , for a given collar width. Nevertheless, both collar shapes around both abutment shapes exhibited decreasing efficiencies with increasing flow intensity and time. On the other hand, at the elevation of  $Z_c/y_{0.7}=-0.25$ , at the initial and final stages of the experiments, the efficiencies of the semi-circular end collars attached to the semi-circular end abutment were observed greater than those of the rectangular collars attached to the rectangular abutment for a given collar width. On the contrary, at the end of the second stage of the experiment with the flow intensity of 0.8, the rectangular collars of  $B_c=7.5$  and 10 cm attached to the rectangular abutment were found to be more effective in reducing the maximum scour depth than the semi-circular end collars attached to the semi-circular end abutment.

Finally, when the collars were placed at the elevation of  $Z_c/y_{0.7}=-0.50$ , the efficiencies of the rectangular collars attached to the rectangular abutment diminished with increasing flow intensity and time. On the contrary, the efficiencies of semi-circular end collars attached to the semi-circular end abutment showed an upward trend over time. Consequently, at the end of 2nd hour with a flow intensity

of 0.7, rectangular collars attached to the rectangular abutment were deemed more efficient for a given collar width at this elevation. However, at the end of the 6th hour after applying each flow intensities of 0.7, 0.8, and 0.9 for 2 h each, semi-circular end collars attached to the semi-circular end abutment were observed as more effective in reducing the maximum scour depth compared to rectangular collars attached to the rectangular abutment for a given collar width. In conclusion, considering the effect of abutment and collar shape on the reduction of maximum scour depth, it can be asserted that semi-circular end collars attached to the semi-circular end abutment exhibit greater effectiveness than rectangular collars attached to the rectangular abutment at the end of the experimental duration of the 6-h under varying flow intensities.

The comparison of the scour reduction performances of the varying collar sizes and elevations around the semi-circular end and rectangular abutments of length  $L_a=30$  cm is presented in Fig. 11 with the data of third stage experiments only.

In Fig. 12, the analysis of the scour reduction performances of different collar sizes and flow intensities around the semi-circular end and rectangular abutments of length  $L_a=30$  cm is illustrated. The results consistently demonstrate that, when the collars were placed at the elevation of  $Z_c/y_{0.7}=\pm 0.00$ , the scour reduction performances of the semi-circular end collars attached to the semi-circular end abutment surpassed those of the rectangular collars attached to the rectangular abutment across all flow intensities and time durations for a given collar width.

On the other hand, at the elevation of  $Z_c/y_{0.7}=-0.25$ , the maximum scour reductions were observed for the rectangular collar of  $B_c=10$  cm attached to the rectangular abutment for all the flow intensities tested. During the first stage of the experiments with a flow intensity of 0.7, the rectangular collars attached to the rectangular abutment exhibited higher efficiency compared to the semi-circular end collars attached to the semi-circular end abutment for a given collar width. Nevertheless, as the flow intensity and time increased, the efficiency of rectangular collars attached to the rectangular abutment decreased. In other words, at the end of the second and third stages of the experiments, at the elevation of  $Z_c/y_{0.7}=-0.25$ , it was shown that the semi-circular end collars attached to semi-circular end abutment were more effective in reducing the maximum scour depth except for the rectangular collar of  $B_c=10$  cm attached to the rectangular abutment.

Finally, when collars were placed at the elevation of  $Z_c/y_{0.7}=-0.50$ , the maximum scour reductions were recorded for the rectangular collars attached to the rectangular abutment for a given collar width and flow intensity.

In Fig. 13, the comparison of the scour reduction performances of the varying collar sizes and elevations around the semi-circular end and rectangular abutments of length

$L_a = 20$  cm is given. At the end of the third stage of the experiments, at the elevation of  $Z_c/y_{0.7} = \pm 0.00$ , the semi-circular end collars attached to semi-circular end abutment gave better performances in reducing the maximum scour depth relative to the rectangular collars attached to the rectangular abutment for a given collar width.

However, when the collars were positioned below the bed level,  $Z_c/y_{0.7} = -0.25$ , the performances of the rectangular collars attached to the rectangular abutment increased while the semi-circular end collars attached to the semi-circular end abutment decreased. At these stages of the experiments, the maximum scour depths were recorded for the semi-circular end collars of  $B_c = 7.5$  and 10 cm attached to semi-circular end abutment at the elevation of  $Z_c/y_{0.7} = \pm 0.00$  while for the rectangular collars of  $B_c = 7.5$  and 10 cm attached to the rectangular abutment at the elevation of  $Z_c/y_{0.7} = -0.25$ .

In Fig. 14, the comparison of scour reduction performances involving various collar sizes and flow intensities around semi-circular end and rectangular abutments of length  $L_a = 20$  cm is depicted. When the collars were placed at the elevation of  $Z_c/y_{0.7} = \pm 0.00$ , the scour reduction performances of the rectangular collars of  $B_c = 7.5$  and 10 cm attached to the rectangular abutment were generally observed greater than those of the semi-circular end collars attached to the semi-circular end abutment during the first 2 h of the experiments having the flow intensity of 0.7. However, as the flow intensity increased, the scour reduction efficiency of the semi-circular end collars attached to the semi-circular end abutment was found to be better when compared to rectangular collars attached to rectangular abutment for a given collar width and flow intensity.

On the other hand, at the elevation of  $Z_c/y_{0.7} = -0.25$ , the rectangular collars attached to the rectangular abutment showed better performances in reducing the maximum scour depth than the semi-circular end collars attached to semi-circular end abutment at any flow intensity tested.

In summary, both semi-circular end and rectangular collars play a crucial role in reducing scour depths around abutments. For the abutment of length  $L_a = 40$  cm, the semi-circular end collars around the semi-circular end abutment consistently exhibited more effective results in reducing the maximum scour depth compared to rectangular collars around rectangular abutments. This situation may be attributed to the sharp characteristics of rectangular abutments, inducing stronger vortices and higher bed shear stress, resulting in more significant scour depths compared to the semi-circular end ones. However, as the abutment length decreased (i.e.,  $L_a = 20$  and 30 cm), the rectangular collars attached to the rectangular abutments gave better performances than the semi-circular collars attached to semi-circular abutments when the collars were placed below the bed level (i.e.,  $Z_c/y_{0.7} = -0.50$  and  $-0.25$ ). Notably, the efficiencies of the rectangular collars attached to rectangular

abutments increased with increasing flow intensity and time. Based on the experimental results, semi-circular collars attached to semi-circular end abutments achieved a reduction in maximum scour depth of up to 72%, while rectangular collars attached to rectangular abutments reduced the maximum scour depth by up to 51%. Table 3 details the ranges of minimum and maximum reductions in maximum scour depths around semi-circular end and rectangular abutments as a function of  $Z_c/y_{0.7}$  and flow intensity.

### Maximum scour depths around the abutments

As an alternative way to demonstrate the relationship between the dimensionless maximum scour depth and abutment-collar sizes, variation of  $[(d_s)_{\max,c}/y]$  and  $\sqrt{\theta(L_a/B_c)}$  is illustrated in Figs. 15 and 16 for the semi-circular end and rectangular abutments, respectively. The  $\theta$  parameter represents the ratio of the total area of the abutment with collar to the area of the abutment on the horizontal plane:

$$\theta = \frac{A_{\text{abutment}} + A_{\text{collar}}}{A_{\text{abutment}}}, \quad (6)$$

where  $A_{\text{abutment}}$  and  $A_{\text{collar}}$  are the areas of the abutment and collar on the plan view, respectively.  $\theta$  values are used to represent the effect of the areal sizes of the abutment models with collars on the reduction of scour around the abutments. The increase in the  $\theta$  value, for a given abutment length, means an increase in the collar width.

Figure 15 shows that the dimensionless maximum scour depth increases with increasing  $\sqrt{\theta(L_a/B_c)}$  for semi-circular end abutments. The general trend of the data points indicated that the dimensionless maximum scour depth increases when the collar was placed below bed level. However, at the end of the third stage, for the  $\sqrt{\theta(L_a/B_c)}$  values greater than 3.80, the collars placed at the elevation of  $Z_c/y_{0.7} = -0.50$  led to smaller maximum scour depths when compared to the collars at the elevation of  $Z_c/y_{0.7} = -0.25$ . Similar to the semi-circular end abutments, the dimensionless maximum scour depth around the rectangular abutments increased with increasing  $\sqrt{\theta(L_a/B_c)}$ .

Figure 16 demonstrates that the dimensionless maximum scour depth around the rectangular abutments generally decreased when the collars were placed below the bed level contrary to the semi-circular end abutments. Only at the end of the first stage of the experiments, the maximum dimensionless scour depths were obtained when the collars were placed at the elevation of  $Z_c/y_{0.7} = -0.50$ .

From Figs. 15 and 16, for known  $\theta$ ,  $L_a/B_c$  and  $Z_c/y_{0.7}$  values within the ranges of this study,  $[(d_s)_{\max,c}/y]$  values can be determined for collar applications on semi-circular end and rectangular abutments. The linear relationships between  $[(d_s)_{\max,c}/y]$  and  $\sqrt{\theta(L_a/B_c)}$  for various flow intensities, collar elevations and test durations are listed in Tables 4 and 5.



Additionally, to illustrate the effect of flow intensity and test duration on the correlation between the dimensionless maximum scour depth and abutment-collar sizes, variation of  $[(d_s)_{\max,c}/y]$  with  $\sqrt{\theta(L_a/B_c)}\exp\left(\frac{U}{U_c}\right)\exp\left(\frac{t}{t_p}\right)$  as a function of collar elevations is presented in Figs. 17 and 18 for the semi-circular end and rectangular abutments, respectively. These figures indicate that the dimensionless maximum scour depths not only increase with increasing abutment size and decreasing collar size but also increase with increasing flow intensity and test duration for both semi-circular end and rectangular abutments at a given collar elevation. Furthermore, as  $\sqrt{\theta(L_a/B_c)}\exp\left(\frac{U}{U_c}\right)\exp\left(\frac{t}{t_p}\right)$  values increased the efficiencies of the collars below the bed level increased due to the greater scour depths observed around longer abutment lengths (i.e.,  $L_a = 40$  cm) and longer test durations with greater flow intensities. For semi-circular end abutments, the maximum dimensionless scour depths generally increased as the collar was located deeper into the bed level as discussed in previous subsections. However, the maximum dimensionless scour depths were observed greater when the collar was placed at the elevation of  $Z_c/y_{0.7} = -0.25$  compared to those at the elevation of  $Z_c/y_{0.7} = -0.50$  in the case of  $\sqrt{\theta(L_a/B_c)}\exp\left(\frac{U}{U_c}\right)\exp\left(\frac{t}{t_p}\right) > 27$ .

On the other hand, for the rectangular abutments, the greatest and lowest maximum dimensionless scour depths were obtained at the elevations of  $Z_c/y_{0.7} = -0.50$  and  $-0.25$ , respectively, for  $\sqrt{\theta(L_a/B_c)}\exp\left(\frac{U}{U_c}\right)\exp\left(\frac{t}{t_p}\right)$

$< 22$ . In addition, in this range, the dimensionless scour depth values at  $Z_c/y_{0.7} = -0.25$  and  $\pm 0.00$  were obtained close to each other. Between the range of  $22 < \sqrt{\theta(L_a/B_c)}\exp\left(\frac{U}{U_c}\right)\exp\left(\frac{t}{t_p}\right) < 25$ , the greatest maximum dimensionless scour depths were obtained at the elevation of  $Z_c/y_{0.7} = \pm 0.00$  while the lowest ones were obtained at the elevation of  $Z_c/y_{0.7} = -0.25$ . Finally, when  $\sqrt{\theta(L_a/B_c)}\exp\left(\frac{U}{U_c}\right)\exp\left(\frac{t}{t_p}\right) > 25$ , again the greatest maximum dimensionless scour depths were obtained at the elevation of  $Z_c/y_{0.7} = \pm 0.00$  and  $-0.50$ , respectively.

## Summary and conclusions

This study investigated the efficacy of collars in reducing scour depths around semi-circular end and rectangular bridge abutments in conditions of unsteady-state clear-water approach flow. A prolonged stepwise hydrograph, simulating a 6-h flood scenario, was employed. This hydrograph, characterized by flow intensity, consisted of three distinct steps, each lasting 2 h. Various sizes of semi-circular end and rectangular collars were positioned at different elevations relative to the bed level around the semi-circular end and rectangular abutments, respectively, to investigate the effect of abutment length, flow intensity, time, collar size, and collar elevation on the scour reduction performances

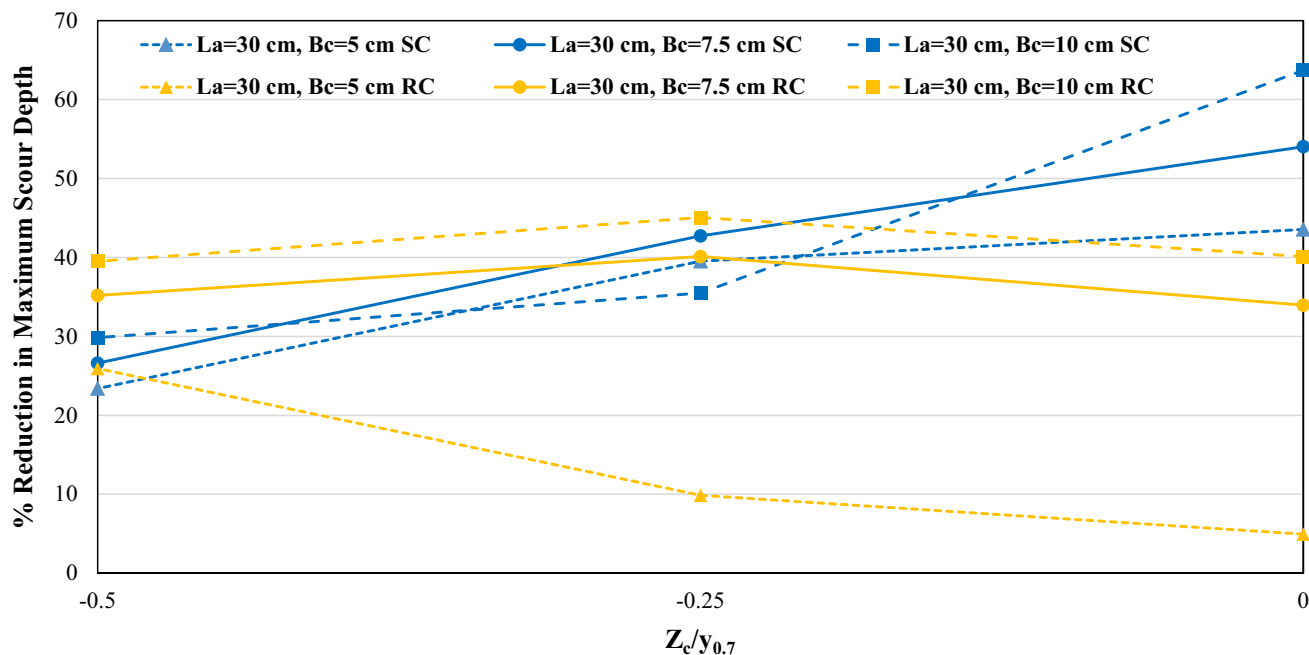


**Fig. 11** Comparison of the effects of collar size and elevation on the maximum scour depth around semi-circular end and rectangular abutments of length  $L_a = 30$  cm ( $t = 6$  h)

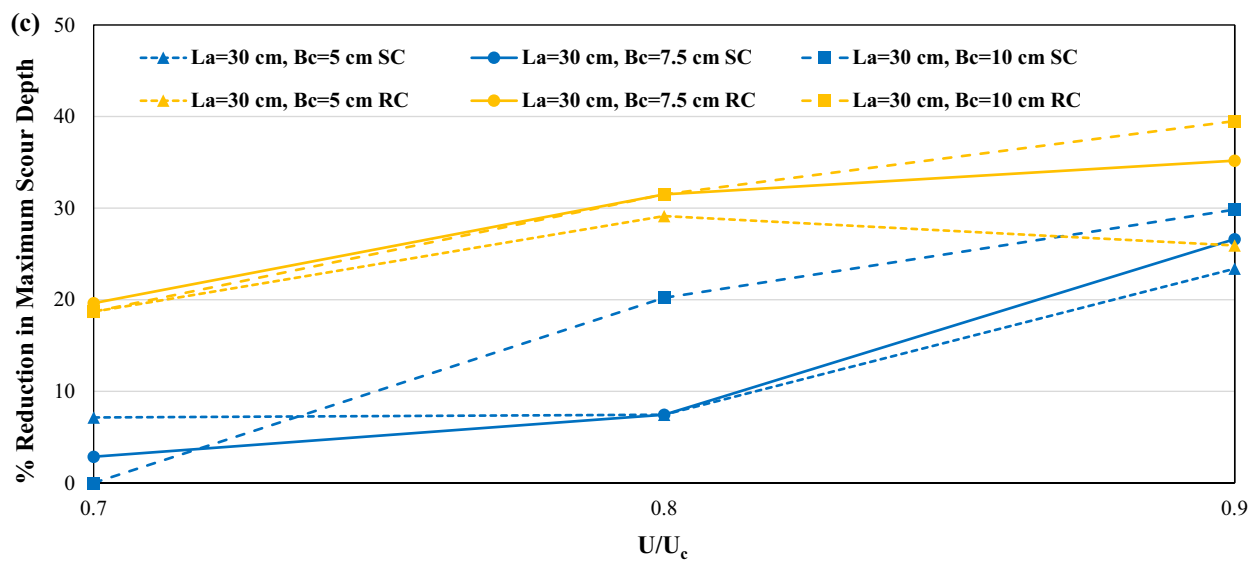
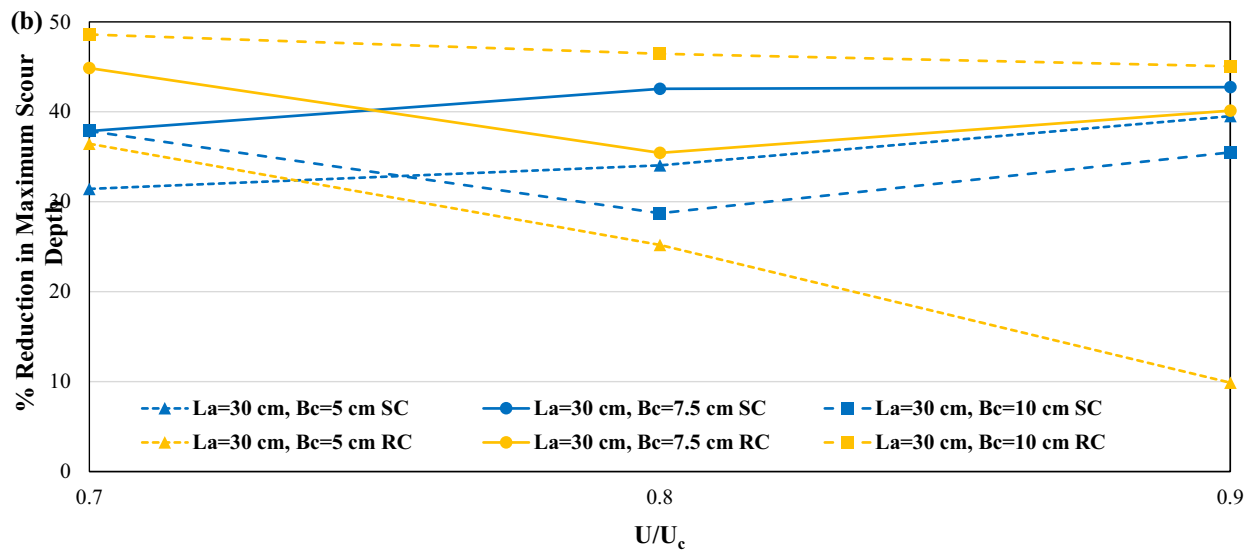
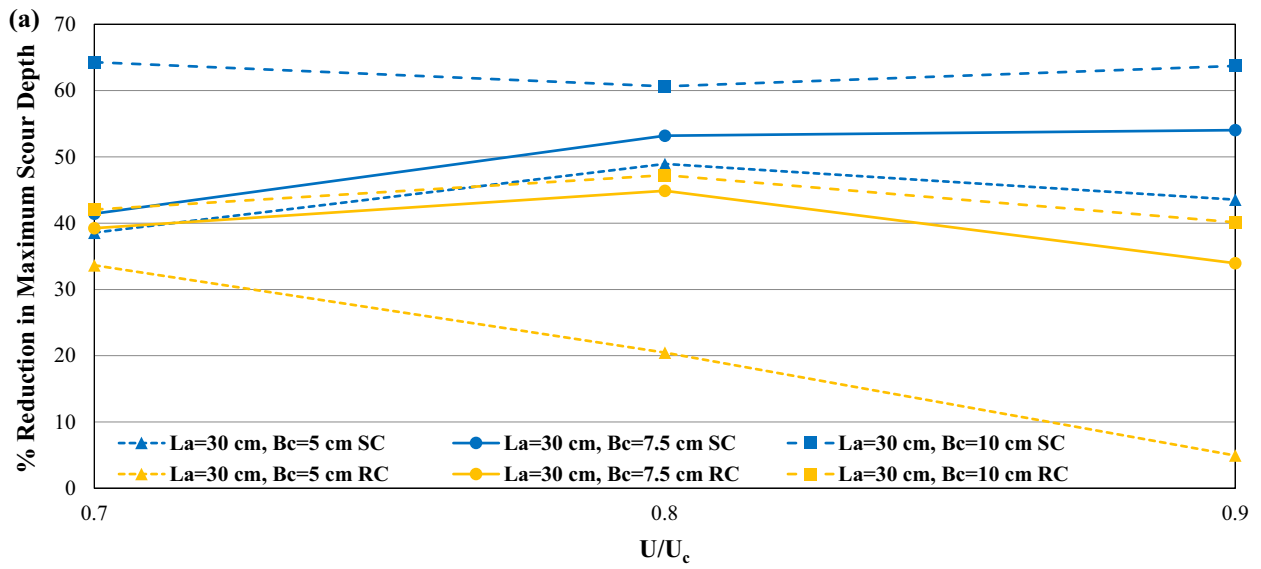


**Fig. 12 a** Comparison of the effect of collar size and flow intensity on the maximum scour depth around semi-circular end and rectangular abutments of length  $L_a=30$  cm for  $Z_c/y_{0.7} = \pm 0.00$ . **b** Comparison of the effect of collar size and flow intensity on the maximum scour depth around semi-circular end and rectangular abutments of length  $L_a=30$  cm for  $Z_c/y_{0.7} = -0.25$ . **c** Comparison of the effect of collar size and flow intensity on the maximum scour depth around semi-circular end and rectangular abutments of length  $L_a=30$  cm for  $Z_c/y_{0.7} = -0.50$

of the collars. The conclusions drawn from this study are listed as follows:

1. A collar attached to a bridge abutment plays a crucial role in diverting the direct force of downward-flowing water, redirecting it toward the sediment. This function can be conceptualized as a mechanism that effectively interrupts the downward movement, akin to a "down-flow-halting" process. This effect becomes especially significant during the initiation of scour holes, where collars serve as a barrier to the development of secondary vortices encircling the abutment, as explained by Li 2005. Consequently, a key observation derived from this investigation highlights the pronounced efficacy of collars as a preventive measure against scour. Their application demonstrates notable success in reducing or preventing scour development around both semi-circular and rectangular abutments.
2. The general trend observed is that with an increase in collar size, the scour reduction efficiencies of the collars tend to increase regardless of the abutment length and shape. This is attributed to the larger collars being more effective in impeding the penetration of vortices into deeper elevations.
3. As the potential for increased scour depths arises due to factors such as much longer abutments, a blunt abutment shape, higher flow intensity values, and extended test duration, the efficiencies of collars positioned below the bed level (i.e.,  $Z_c/y_{0.7} = -0.50$  and  $-0.25$ ) increased. However, for the smaller scour depth potential, the collars placed at the bed level,  $Z_c/y_{0.7} = \pm 0.00$  were found to be better in reducing the maximum scour depths around the abutments. Consequently, for the semi-circular end abutments tested in this study, the most efficient collar performances were generally observed when the collars were placed at the elevation of  $Z_c/y_{0.7} = \pm 0.00$ . On the contrary, the collars were placed at the elevations of  $Z_c/y_{0.7} = -0.50$  and  $-0.25$  generally gave better results in reducing the maximum scour depth for rectangular abutments.
4. The scour reduction performances of the collars at the elevations of  $Z_c/y_{0.7} = -0.25$  and  $\pm 0.00$  generally decreased with increasing flow intensity and test duration regardless of the abutment shape while at the elevation of  $Z_c/y_{0.7} = -0.50$  increased.

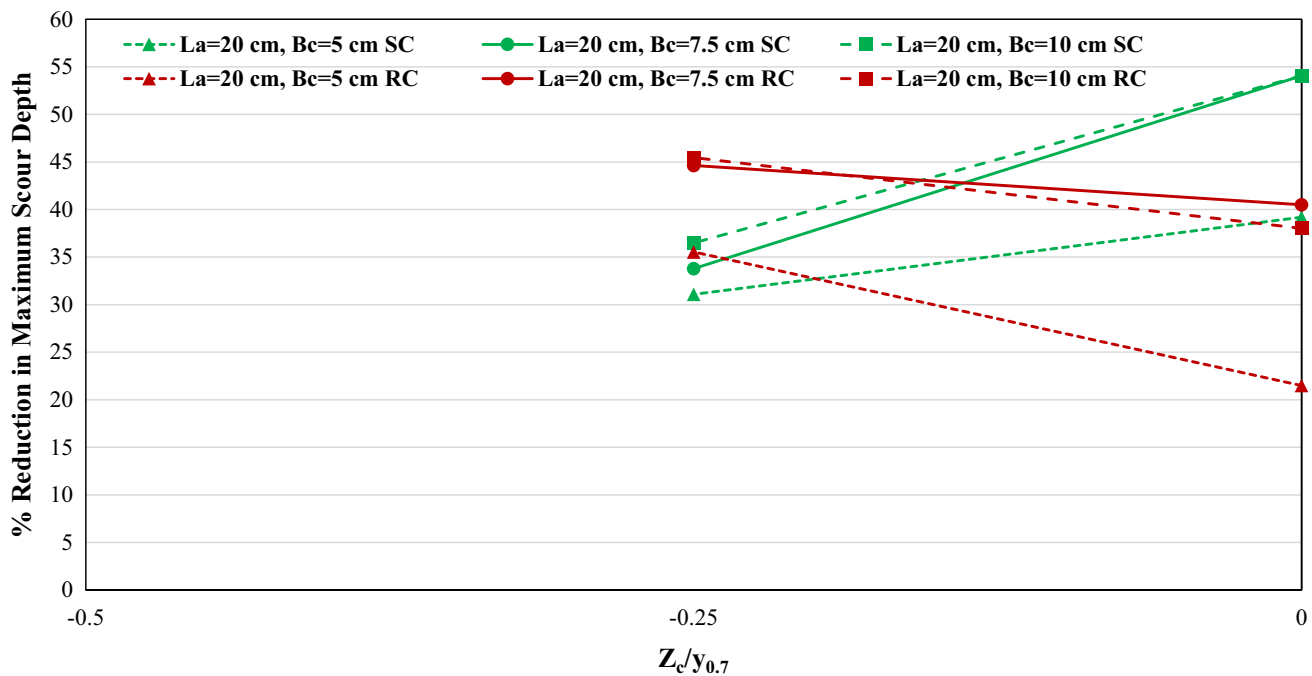


**Fig. 13** Comparison of the effects of collar size and elevation on the maximum scour depth around semi-circular end and rectangular abutments of length  $L_a=20$  cm ( $t=6$  h)

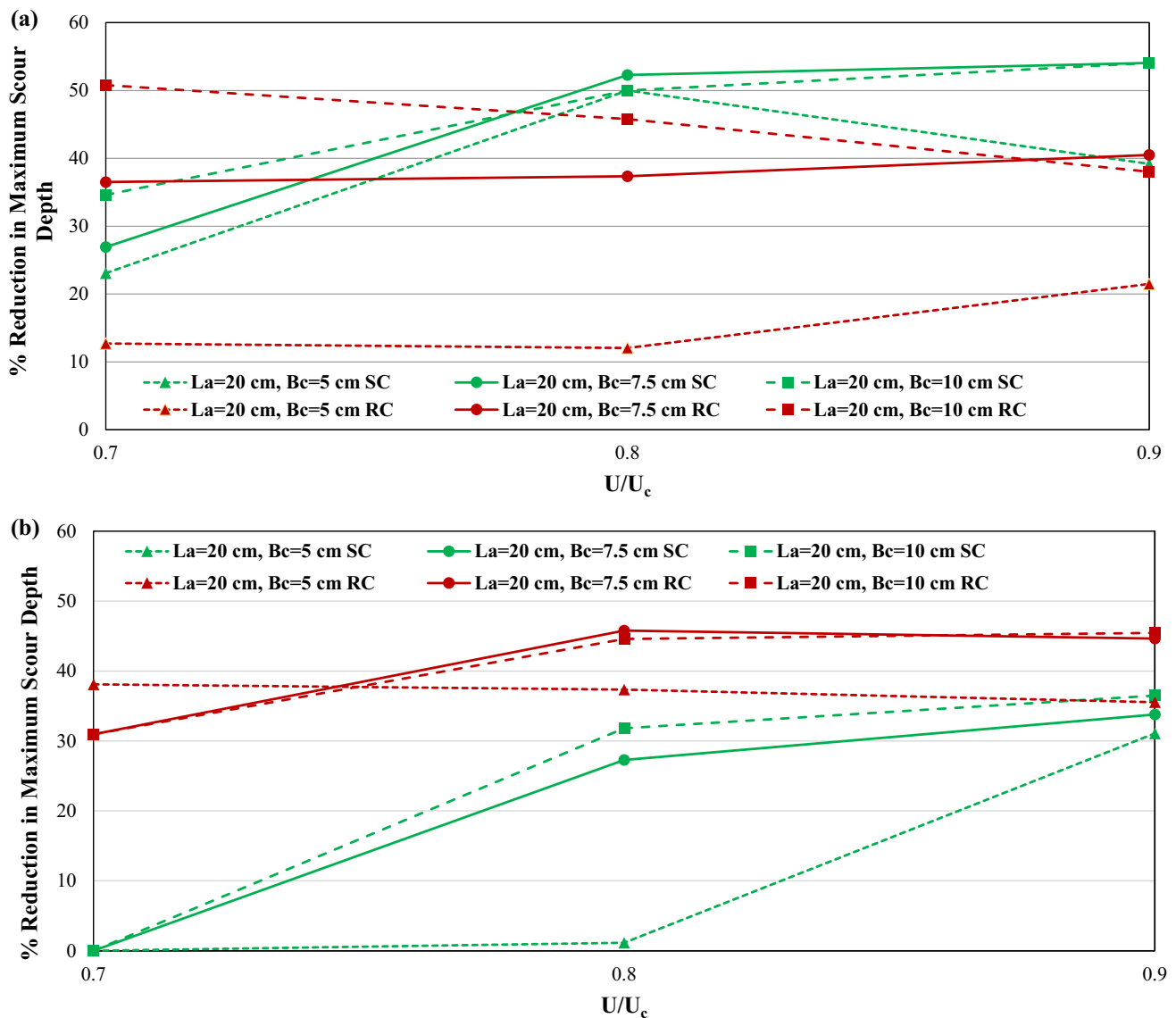


**Fig. 14 a** Comparison of the effect of collar size and flow intensity on the maximum scour depth around semi-circular end and rectangular abutments of length  $L_a = 20$  cm for  $Z_c/y_{0.7} = \pm 0.00$ . **b** Comparison

of the effect of collar size and flow intensity on the maximum scour depth around semi-circular end and rectangular abutments of length  $L_a = 20$  cm for  $Z_c/y_{0.7} = -0.25$

- Based on the experimental findings, the semi-circular end collars, when placed around semi-circular end abutments, demonstrated a scour depth reduction of up to approximately 72%, whereas rectangular collars around rectangular abutments achieved a reduction of around 52%.
- The dimensionless maximum scour depth with a collar,  $[(d_s)_{\max,c}/y]$ , increased regardless of abutment shape, flow intensity and test duration with increasing  $\sqrt{\theta(L_a/B_c)}$  value, where  $L_a/B_c$  denotes the abutment length and collar size ratio and  $\theta$  present the effect of areal sizes of the abutment models with collars on the reduction of maximum scour around the abutments.

Also, the linear relationships between  $[(d_s)_{\max,c}/y]$  and  $\sqrt{\theta(L_a/B_c)}$  with varying flow intensities, collar elevations and test durations are listed in Tables 4 and 5.

- Variation of  $[(d_s)_{\max,c}/y]$  and  $\sqrt{\theta(L_a/B_c)} \exp\left(\frac{U}{U_c}\right) \exp\left(\frac{t}{t_p}\right)$  shown in Figs. 17 and 18 for the semi-circular end and rectangular abutments showed that the efficiencies of the collars located below the bed level increased as  $\sqrt{\theta(L_a/B_c)} \exp\left(\frac{U}{U_c}\right) \exp\left(\frac{t}{t_p}\right)$  values increased.

As part of abutment scour and its countermeasures techniques there are still a number of interesting subjects that

**Table 3** The ranges of minimum and maximum % reductions in maximum scour depths around semi-circular end and rectangular abutments tested

		$2.0 \leq L_a/B_c \leq 8.0$		The range of % reduction in maximum scour depth	
$Z_c/y_{0.7}$	$t$ (hour)	$U/U_c$	Semi-circular end collars attached to the semi-circular end abutments	Rectangular collars attached to the rectangular abutments	
±0.00	2	0.7	23.08–71.88	12.70–50.79	
	4	0.8	28.46–62.31	8.19–47.24	
	6	0.9	22.36–63.71	0.48–40.50	
−0.25	2	0.7	0.00–50.00	30.95–48.60	
	4	0.8	1.14–42.55	25.20–47.37	
	6	0.9	19.25–42.74	1.90–45.45	
−0.50	2	0.7	0.00–9.38	18.69–36.84	
	4	0.8	7.45–30.77	27.49–39.18	
	6	0.9	23.39–33.54	10.95–39.51	

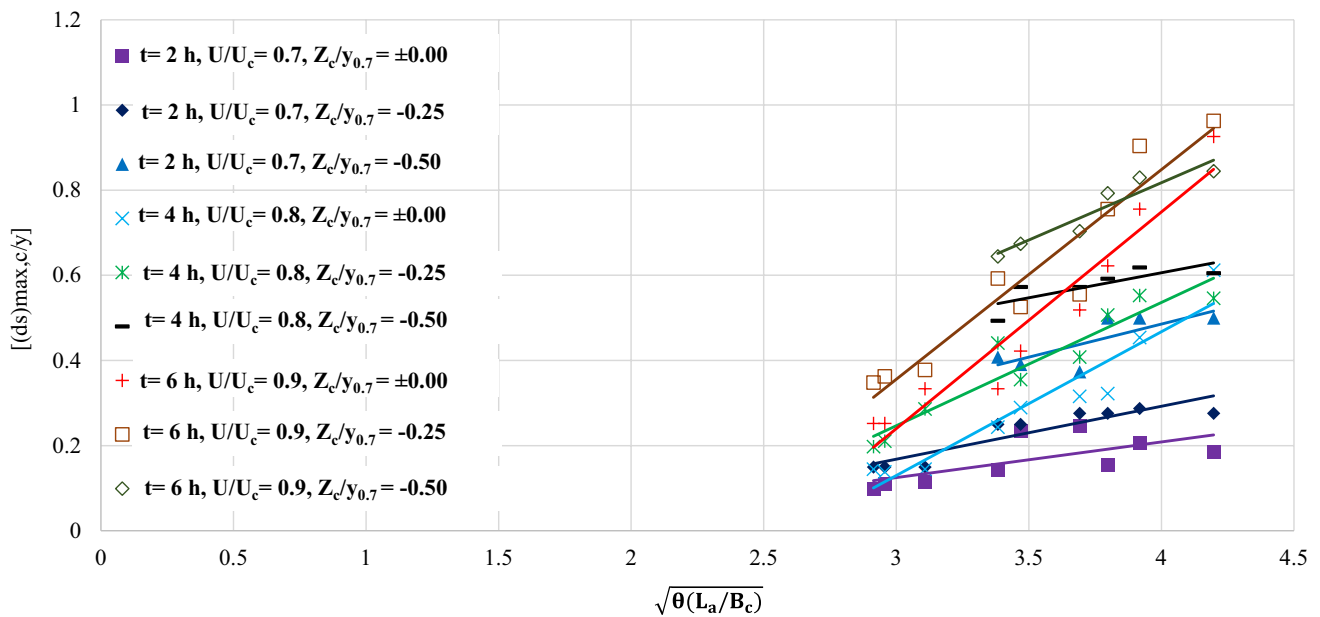


**Fig. 15** Variation of  $[(d_s)_{max,c}/y]$  with  $\sqrt{\theta(L_a/B_c)}$  for semi-circular end abutments

warrant additional research. Some of them are provided below for potential future research:

1. Current studies in the literature have been mainly carried out under clear-water scour conditions rather than live-bed scour conditions. To get a better understanding of the abutment scour and the efficiency of its countermeasures, experiments should be conducted under live-bed scour conditions.
2. It is important to test and compare the scour reduction efficiencies of the recently introduced collar shapes such as airfoil and streamlined shapes, with those of the traditional ones, including rectangular and semi-circular end collars.
3. The scour reduction performances of various flow-altering countermeasures, such as slots and vanes, should also be examined under unsteady-state flow conditions.

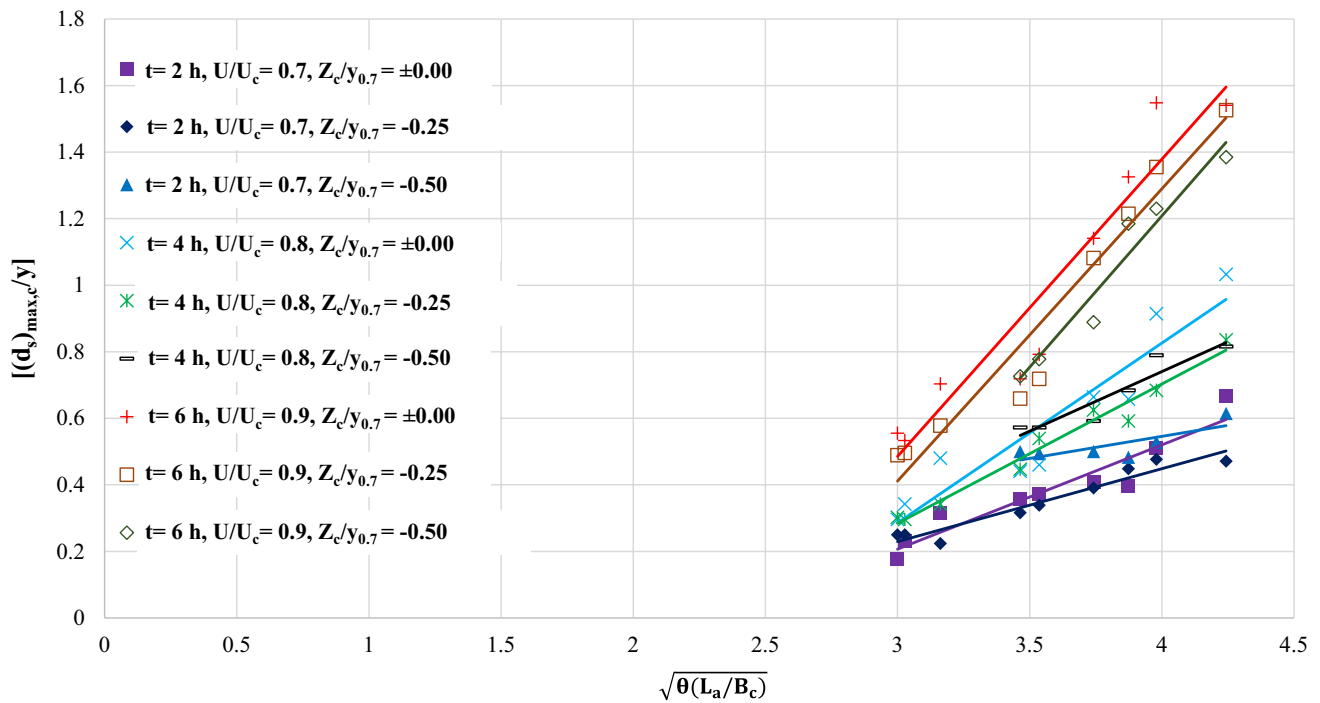


**Fig. 16** Variation of  $[(d_s)_{\max,c}/y]$  with  $\sqrt{\theta(L_a/B_c)}$  for rectangular abutments

**Table 4** The linear relationships between  $[(d_s)_{\max,c}/y]$  and  $\sqrt{\theta(L_a/B_c)}$  for semi-circular end abutments with varying flow intensities, collar elevations and test durations

	Equation	$R^2$
$t=2 \text{ h}, U/U_c=0.7, Z_c/y_{0.7}=\pm 0.00$	$[(d_s)_{\max,c}/y] = 0.0837\sqrt{\theta\left(\frac{L_a}{B_c}\right)} - 0.1264$	0.4548
$t=2 \text{ h}, U/U_c=0.7, Z_c/y_{0.7}=-0.25$	$[(d_s)_{\max,c}/y] = 0.1243\sqrt{\theta\left(\frac{L_a}{B_c}\right)} - 0.205$	0.8239
$t=2 \text{ h}, U/U_c=0.7, Z_c/y_{0.7}=-0.50$	$[(d_s)_{\max,c}/y] = 0.1553\sqrt{\theta\left(\frac{L_a}{B_c}\right)} - 0.1358$	0.5831
$t=4 \text{ h}, U/U_c=0.8, Z_c/y_{0.7}=\pm 0.00$	$[(d_s)_{\max,c}/y] = 0.3378\sqrt{\theta\left(\frac{L_a}{B_c}\right)} - 0.8836$	0.9117
$t=4 \text{ h}, U/U_c=0.8, Z_c/y_{0.7}=-0.25$	$[(d_s)_{\max,c}/y] = 0.2895\sqrt{\theta\left(\frac{L_a}{B_c}\right)} - 0.622$	0.8984
$t=4 \text{ h}, U/U_c=0.8, Z_c/y_{0.7}=-0.50$	$[(d_s)_{\max,c}/y] = 0.1175\sqrt{\theta\left(\frac{L_a}{B_c}\right)} + 0.1359$	0.6321
$t=6 \text{ h}, U/U_c=0.9, Z_c/y_{0.7}=\pm 0.00$	$[(d_s)_{\max,c}/y] = 0.5089\sqrt{\theta\left(\frac{L_a}{B_c}\right)} - 1.2871$	0.9250
$t=6 \text{ h}, U/U_c=0.9, Z_c/y_{0.7}=-0.25$	$[(d_s)_{\max,c}/y] = 0.4925\sqrt{\theta\left(\frac{L_a}{B_c}\right)} - 1.1217$	0.9095
$t=6 \text{ h}, U/U_c=0.9, Z_c/y_{0.7}=-0.50$	$[(d_s)_{\max,c}/y] = 0.2692\sqrt{\theta\left(\frac{L_a}{B_c}\right)} - 0.2593$	0.8969

**Table 5** The linear relationships between  $[(d_s)_{\max,c}/y]$  and  $\sqrt{\theta(L_a/B_c)}$  for rectangular abutments with varying flow intensities, collar elevations and test durations

	Equation	$R^2$
$t=2$ h, $U/U_c=0.7$ , $Z_c/y_{0.7}=\pm 0.00$	$[(d_s)_{\max,c}/y] = 0.3134\sqrt{\theta\left(\frac{L_a}{B_c}\right)} - 0.7334$	0.8966
$t=2$ h, $U/U_c=0.7$ , $Z_c/y_{0.7}=-0.25$	$[(d_s)_{\max,c}/y] = 0.2192\sqrt{\theta\left(\frac{L_a}{B_c}\right)} - 0.4281$	0.9323
$t=2$ h, $U/U_c=0.7$ , $Z_c/y_{0.7}=-0.50$	$[(d_s)_{\max,c}/y] = 0.1325\sqrt{\theta\left(\frac{L_a}{B_c}\right)} + 0.0158$	0.6166
$t=4$ h, $U/U_c=0.8$ , $Z_c/y_{0.7}=\pm 0.00$	$[(d_s)_{\max,c}/y] = 0.3378\sqrt{\theta\left(\frac{L_a}{B_c}\right)} - 0.8836$	0.9117
$t=4$ h, $U/U_c=0.8$ , $Z_c/y_{0.7}=-0.25$	$[(d_s)_{\max,c}/y] = 0.4189\sqrt{\theta\left(\frac{L_a}{B_c}\right)} - 0.9722$	0.9723
$t=4$ h, $U/U_c=0.8$ , $Z_c/y_{0.7}=-0.50$	$[(d_s)_{\max,c}/y] = 0.3580\sqrt{\theta\left(\frac{L_a}{B_c}\right)} + 0.6913$	0.8828
$t=6$ h, $U/U_c=0.9$ , $Z_c/y_{0.7}=\pm 0.00$	$[(d_s)_{\max,c}/y] = 0.8933\sqrt{\theta\left(\frac{L_a}{B_c}\right)} - 2.1943$	0.9142
$t=6$ h, $U/U_c=0.9$ , $Z_c/y_{0.7}=-0.25$	$[(d_s)_{\max,c}/y] = 0.8784\sqrt{\theta\left(\frac{L_a}{B_c}\right)} - 2.2236$	0.9430
$t=6$ h, $U/U_c=0.9$ , $Z_c/y_{0.7}=-0.50$	$[(d_s)_{\max,c}/y] = 0.9094\sqrt{\theta\left(\frac{L_a}{B_c}\right)} - 2.429$	0.9473

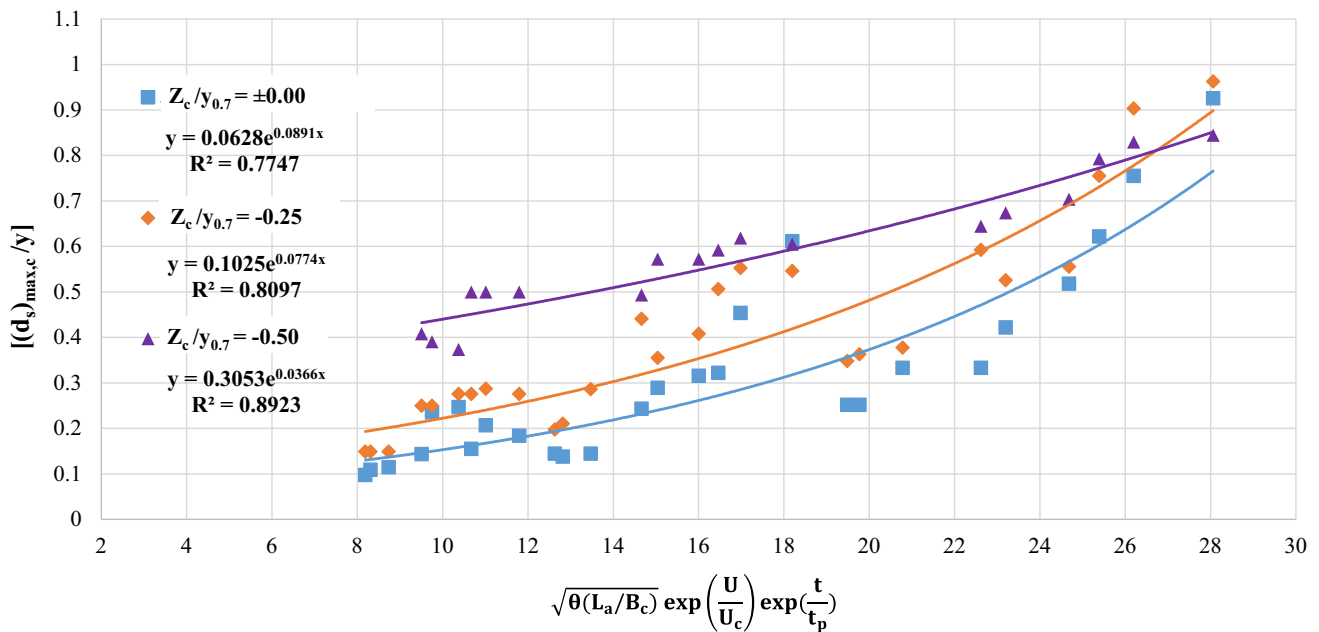


**Fig. 17** Variation of  $[(d_s)_{\max,c}/y]$  with  $\sqrt{\theta(L_a/B_c)}\exp\left(\frac{U}{U_c}\right)\exp\left(\frac{t}{t_p}\right)$  for semi-circular end abutments

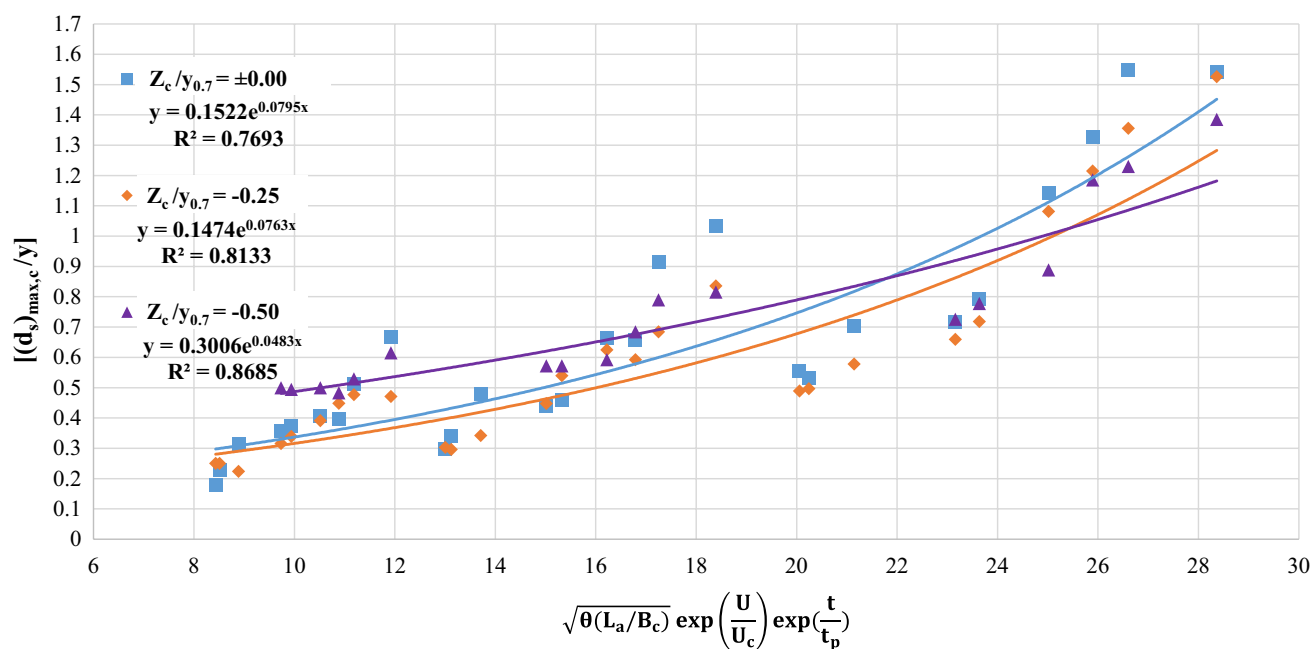


**Fig. 18** Variation of  $[(d_s)_{\max,c}/y]$  with  $\sqrt{\theta(L_a/B_c)} \exp\left(\frac{U}{U_c}\right) \exp\left(\frac{t}{t_p}\right)$  for rectangular abutments

**Acknowledgements** There is not any acknowledgement.

**Author contributions** Conceptualization done by MG; methodology done by SG and MG; formal analysis and investigation done by SG; writing—original draft preparation done by SG, MG, and ABA-S; writing—review and editing done by SG, MG, and ABA-S; supervision done by Mustafa Gogus and ABA-S.

**Funding** This research did not receive any specific grant from funding agencies in the public, commercial, or not-for-profit sectors.

**Data availability** The experimental data would be available upon a reasonable request.

**Code availability** Not applicable.

## Declarations

**Conflicts of interest** The authors have no competing interests to declare that are relevant to the content of this article.

## References

- Alabi PD (2006) Time development of local scour at a bridge pier fitted with a collar. Master Thesis, University of Saskatchewan
- Bombar G (2020) Scour evolution around bridge piers under hydrographs with high unsteadiness. Iran J Sci Technol Trans Civ Eng 44:325–337. <https://doi.org/10.1007/s40996-019-00321-8>
- Barbhuiya AK, Dey S (2004) Local scour at abutments: a review. Sadhana 29:449–476. <https://doi.org/10.1007/BF02703255>
- Borghai SM, Kabiri-Samani A, Banihashem SA (2012) Influence of unsteady flow hydrograph shape on local scouring around bridge pier. Proc Inst Civ Eng Water Manag 165:473–480. <https://doi.org/10.1680/wama.11.00020>
- Cao X, Gu Z (2015) Three classification criteria and their comparison impact scale between double non-submerged spur dikes. J Zhejiang Univ 49:200–207
- Coleman SE, Lauchlan CS, Melville BW (2003) Développement de l'affouillement en eau claire aux butées de pont. J Hydraul Res 41:521–531. <https://doi.org/10.1080/00221680309499997>
- Dey S, Barbhuiya AK (2005) Time variation of scour at abutments. J Hydraul Eng 131:11–23. [https://doi.org/10.1061/\(asce\)0733-9429\(2005\)131:1\(11\)](https://doi.org/10.1061/(asce)0733-9429(2005)131:1(11))
- Dey Subhasish B, Sumer M, Fredsøe J (2006) Control of scour at vertical circular piles under waves and current. J Hydraul Eng 132:270–279. <https://doi.org/10.1061/ASCE0733-94292006132:3270>
- Farshad R, Kashefipour SM, Ghomeshi M, Oliveto G (2022) Temporal scour variations at permeable and angled spur dikes under steady and unsteady flows. Water (switzerland) 14:3310. <https://doi.org/10.3390/w14203310>
- Gökmener S (2023) Effect of flow intensity and collars on scour depths around bridge abutments. Doctoral Thesis, Middle East Technical University
- Gogus M, Dogan AE (2010) Effects of collars on scour reduction at bridge abutments. In: Scour and Erosion. pp 997–1007
- Gokmener S, Gogus M (2022) Local scour evolution around semi-circular end bridge abutment in quasi-unsteady condition. Proc Inst Civ Eng Water Manag 175:163–177. <https://doi.org/10.1680/jwama.20.00072>
- Gaudio R, Tafarjnoruz A, Calomino F (2012) Combined flow-altering countermeasures against bridge pier scour. J Hydraul Res 50:35–43. <https://doi.org/10.1080/00221686.2011.649548>
- Grimaldi C, Gaudio R, Calomino F, Cardoso AH (2009) Countermeasures against local scouring at bridge piers: slot and combined system of slot and bed sill. J Hydraul Eng 135:425–431. <https://doi.org/10.1061/ASCEHY.1943-7900.0000035>
- Gu Z, Cao X, Gu Q, Lu WZ (2020) Exploring proper spacing threshold of non-submerged spur dikes with ipsilateral layout. Water (switzerland) 12:172. <https://doi.org/10.3390/w12010172>



- Gogus M, Daskin S, Gokmener S (2023) Effects of collars on local scour around semi-circular end bridge abutments. *Proc Inst Civ Eng Water Manag*. <https://doi.org/10.1680/jwama.21.00011>
- Gupta LK, Pandey M, Anand Raj P (2023a) Numerical simulation of local scour around the pier with and without airfoil collar (AFC) using FLOW-3D. *Environ Fluid Mech*. <https://doi.org/10.1007/s10652-023-09932-2>
- Gupta LK, Pandey M, Raj PA (2023b) Impact of airfoil collar on scour reduction around the bridge pier. *Ocean Eng* 290:116271. <https://doi.org/10.1016/j.oceaneng.2023.116271>
- Gupta LK, Pandey M, Raj PA, Pu JH (2023c) Scour reduction around bridge pier using the airfoil-shaped collar. *Hydrology* 10:77. <https://doi.org/10.3390/hydrology10040077>
- Hager WH, Unger J (2010) Bridge pier scour under flood waves. *J Hydraul Eng* 136:842–847. <https://doi.org/10.1061/ASCEHY.1943-7900.0000281>
- Hosseinjanzadeh H, Khozani ZS, Ardeshtir A, Singh VP (2021) Experimental investigation into the use of collar for reducing scouring around short abutments. *ISH J Hydraul Eng* 27:616–632
- Imhof D (2004) Risk assessment of existing bridge structures. Doctoral Thesis, University of Cambridge
- Johnson PA, Hey RD, Tessier M, Rosgen DL (2001) Use of vanes for control of scour at vertical wall abutments. *J Hydraul Eng* 127:772–778
- Kandasamy JK, Melville BW (1998) Maximum local scour depth at bridge piers and abutments. *J Hydraul Res* 36:183–198. <https://doi.org/10.1080/00221689809498632>
- Kassem H, El-Masry AA, Diab R (2023) Influence of collar's shape on scour hole geometry at circular pier. *Ocean Eng* 287:115791. <https://doi.org/10.1016/j.oceaneng.2023.115791>
- Khosravinia P, Malekpour A, Hosseinzadehdalir A, Farsadizadeh D (2018) Effect of trapezoidal collars as a scour countermeasure around wing-wall abutments. *Water Sci Eng* 11:53–60. <https://doi.org/10.1016/j.wse.2018.03.001>
- Kothiyari UC, Ranga Raju KG (2001) Scour around spur dikes and bridge abutments. *J Hydraul Res* 39:367–374. <https://doi.org/10.1080/00221680109499841>
- Kumar V, Ranga Raju KG, Vittal N (1999) Reduction of local scour around bridge piers using slots and collars. *J Hydraul Eng* 125:1302–1305. [https://doi.org/10.1061/\(ASCE\)0733-9429\(1999\)125:12\(1302\)](https://doi.org/10.1061/(ASCE)0733-9429(1999)125:12(1302))
- Kumcu ŞY, Göğüş M, Kökpinar MA (2007) Temporal scour development at bridge abutments with a collar. *Can J Civ Eng* 34:549–556. <https://doi.org/10.1139/L06-146>
- Kumcu SY, Kokpinar MA, Gogus M (2014) Scour protection around vertical-wall bridge abutments with collars. *KSCE J Civ Eng* 18:1884–1895. <https://doi.org/10.1007/s12205-014-0245-4>
- Li H (2005) Countermeasures against scour at bridge abutments. Doctoral Thesis, Michigan Technological University
- Li H, Barkdoll B, Kuhnle R (2005) Bridge abutment collar as a scour countermeasure. In: *Impacts of global climate change*. pp 1–12
- Li H, Kuhnle RA, Barkdoll BD (2006) Countermeasures against scour at abutments. National Sedimentation Laboratory
- Melville BW (1992) Local scour at bridge abutments. *J Hydraul Eng* 118:615–631. [https://doi.org/10.1061/\(ASCE\)0733-9429\(1992\)118:4\(615\)](https://doi.org/10.1061/(ASCE)0733-9429(1992)118:4(615))
- Melville BW, Chiew Y-M (1999) Time scale for local scour at bridge piers. *J Hydraul Eng* 125:59–65. [https://doi.org/10.1061/\(ASCE\)0733-9429\(1999\)125:1\(59\)](https://doi.org/10.1061/(ASCE)0733-9429(1999)125:1(59))
- Melville BW, Coleman SE (2000) Bridge scour. Water Resources Publication
- Moncada-M AT, Aguirre-Pe J, Bolívar JC, Flores EJ (2009) Scour protection of circular bridge piers with collars and slots. *J Hydraul Res* 47:119–126. <https://doi.org/10.3826/jhr.2009.3244>
- Mashahir M, Zarrati AR, Karimaei Tabarestani M (2024) Evaluation of collar efficiency to prevent scouring around cylindrical bridge piers under live bed condition. *J Hydro-Environ Res* 52:17–25. <https://doi.org/10.1016/j.jher.2023.12.001>
- Oliveto G, Hager WH (2002) Temporal evolution of clear-water pier and abutment scour. *J Hydraul Eng* 128:811–820. <https://doi.org/10.1061/ASCE0733-94292002128:9811>
- Oliveto G, Hager WH (2005) Further results to time-dependent local scour at bridge elements. *J Hydraul Eng* 131:97–105. [https://doi.org/10.1061/\(asce\)0733-9429\(2005\)131:2\(97\)](https://doi.org/10.1061/(asce)0733-9429(2005)131:2(97))
- Pandey M, Azamathulla HM, Chaudhuri S et al (2020) Reduction of time-dependent scour around piers using collars. *Ocean Eng* 213:107692. <https://doi.org/10.1016/j.oceaneng.2020.107692>
- Richardson EV, Davis SR (2001) Evaluating scour at bridges (No. FHWA-NHI-01-001). United States. Federal Highway Administration. Office of Bridge. Technology (Singap World Sci)
- Raikaer RV, Hong JH, Deshmukh AR, Guo WD (2022) Parametric study on abutment scour under unsteady flow. *Water (switzerland)* 14:1820. <https://doi.org/10.3390/w14111820>
- Shampa, Hasegawa Y, Nakagawa H et al (2020) Three-dimensional flow characteristics in slit-type permeable spur dike fields: efficacy in riverbank protection. *Water (switzerland)* 12:964. <https://doi.org/10.3390/W12040964>
- Tekin F (2012) Local scour characteristics around semi-circular end bridge abutments with and without collars. Master Thesis, Middle East Technical University
- Tabarestani MK, Zarrati AR (2017) Local scour calculation around bridge pier during flood event. *KSCE J Civ Eng* 21:1462–1472. <https://doi.org/10.1007/s12205-016-0986-3>
- Tabarestani MK, Zarrati AR (2019) Local scour depth at a bridge pier protected by a collar in steady and unsteady flow. *Proc Inst Civ Eng Water Manag* 172:301–311. <https://doi.org/10.1680/jwama.18.00061>
- Tafarojnouruz A, Gaudio R, Dey S (2010) Flow-altering countermeasures against scour at bridge piers: a review. *J Hydraul Res* 48:441–452. <https://doi.org/10.1080/00221686.2010.491645>
- Tafarojnouruz A, Gaudio R, Calomino F (2012) Evaluation of flow-altering countermeasures against bridge pier scour. *J Hydraul Eng* 138:297–305. [https://doi.org/10.1061/\(asce\)hy.1943-7900.0000512](https://doi.org/10.1061/(asce)hy.1943-7900.0000512)
- Valela C, Nistor I, Rennie CD et al (2021) Hybrid modeling for design of a novel bridge pier collar for reducing scour. *J Hydraul Eng* 147:04021012. [https://doi.org/10.1061/\(asce\)hy.1943-7900.0001875](https://doi.org/10.1061/(asce)hy.1943-7900.0001875)
- Valela C, Rennie CD, Nistor I (2022) Improved bridge pier collar for reducing scour. *Int J Sedim Res* 37:37–46. <https://doi.org/10.1016/j.ijsrc.2021.04.004>
- Wang C, Yu X, Liang F (2017) A review of bridge scour: mechanism, estimation, monitoring and countermeasures. *Nat Hazards* 87:1881–1906. <https://doi.org/10.1007/s11069-017-2842-2>
- Wang S, Wei K, Shen Z, Xiang Q (2019) Experimental investigation of local scour protection for cylindrical bridge piers using anti-scour collars. *Water (switzerland)* 11:1515. <https://doi.org/10.3390/w11071515>
- Yilmaz K (2014) Application of collars as a scour countermeasure for spill-through abutments. Master Thesis, Middle East Technical University
- Zarrati AR, Chamani MR, Shafaie A, Latifi M (2010) Scour countermeasures for cylindrical piers using riprap and combination of collar and riprap. *Int J Sediment Res* 25:313–322. [https://doi.org/10.1016/S1001-6279\(10\)60048-0](https://doi.org/10.1016/S1001-6279(10)60048-0)
- Zarrati AR, Gholami H, Mashahir MB (2004) Application of collar to control scouring around rectangular bridge piers. *J Hydraul Res*. <https://doi.org/10.1080/00221686.2004.9641188>

Springer Nature or its licensor (e.g. a society or other partner) holds exclusive rights to this article under a publishing agreement with the author(s) or other rightsholder(s); author self-archiving of the accepted manuscript version of this article is solely governed by the terms of such publishing agreement and applicable law.